

1 **Millennial-scale variations of sedimentary oxygenation in the western**
2 **subtropical North Pacific and its links to the North Atlantic climate**

3
4 Jianjun Zou^{1,2}, Xuefa Shi^{1,2}, Aimei Zhu¹, Selvaraj Kandasamy³, Xun Gong⁴, Lester
5 Lembke-Jene⁴, Min-Te Chen⁵, Yonghua Wu^{1,2}, Shulan Ge^{1,2}, Yanguang Liu^{1,2}, Xinru
6 Xue¹, Gerrit Lohmann⁴, Ralf Tiedemann⁴

7 ¹Key Laboratory of Marine Sedimentology and Environmental Geology, First Institute
8 of Oceanography, MNR, Qingdao 266061, China

9 ²Laboratory for Marine Geology, Qingdao National Laboratory for Marine Science
10 and Technology, Qingdao, 266061, China

11 ³Department of Geological Oceanography and State Key Laboratory of Marine
12 Environmental Science, Xiamen University, Xiamen361102, China

13 ⁴Alfred-Wegener-Institut Helmholtz-Zentrum für Polar- und Meeresforschung,
14 Bussestr. 24, 27570 Bremerhaven, Germany

15 ⁵Institute of Applied Geosciences, National Taiwan Ocean University, Keelung 20224,
16 Taiwan

17
18 Corresponding authors:

19 Jianjun Zou (zoujianjun@fio.org.cn); Xuefa Shi (xfshi@fio.org.cn)

20
21 **Key Points**

22 **1. This study reconstructs the History-history of sedimentary oxygenation processes at**
23 **mid-depths in the western subtropical North Pacific since the Last last gGlacial period**
24 **is reconstructed using sediment bound geochemical proxies.**

25 **2. Sediment-bound rRedox-sensitive proxies reveal millennial-scale variations in**
26 **sedimentary oxygenation that correlated closely to changes in the North Pacific**
27 **Intermediate Water.**

28 **3. A millennial-scale out-of-phase relationship between deglacial ventilation in the**
29 **western subtropical North Pacific and the formation of North Atlantic Deep Water is**
30 **suggested.**

带格式的: 无下划线, 字体颜色: 自动设置

31 | 4. A larger CO₂ storage at mid-depths of the North Pacific corresponds to the
32 | termination of atmospheric CO₂ rise during the Bölling-Alleröd interval.

33

带格式的: 无下划线, 字体颜色: 自动设置

Abstract

~~Deep ocean carbon cycle, especially carbon sequestration and outgassing, is one of the competitive mechanisms to explain variations in Lower glacial atmospheric CO₂ concentrations on orbital and millennial timescales have been attributed to carbon sequestration in deep oceans.~~ However, ~~the~~ potential roles of ~~voluminous~~ subtropical North Pacific subsurface waters in modulating atmospheric CO₂ levels on millennial timescales ~~are~~ is poorly constrained. Further, an increase in respired CO₂ concentration in the glacial deep ocean due to biological pump generally ~~is coeval with~~ corresponds to less deoxygenation in the subsurface layer. This link thus offers a chance to visit oceanic ventilation and the coeval export productivity based on redox-controlled, sedimentary geochemical parameters. Here we investigate a suite of ~~sediment~~ geochemical proxies in a sediment core CSH1 to understand the sedimentary oxygenation variations in the subtropical North Pacific ~~(core CSH1)~~ over the last 50 thousand years (ka). Our results suggest that enhanced sedimentary oxygenation at mid-depths of the subtropical North Pacific ~~intensifies~~ occurred during the cold interval ~~episodes of late glacial (50-25 ka), Last Glacial Maximum (LGM) and also the interval~~ after 8.5 ka, while decreased oxygenation during the Bölling-Alleröd (B/A) and Preboreal. ~~The especially pronounced for the North Atlantic millennial scale abrupt cold events of the Younger Dryas, Heinrich Stadial (HS) 1 and 2. On the other hand, oxygen depleted seawater is found during the Bölling-Alleröd (B/A) and Preboreal. Our findings of~~ enhanced sedimentary oxygenation in the subtropical North Pacific is aligned with intensified formation of North Pacific Intermediate Water (NPIW) during cold spells, while the ameliorated sedimentary oxygenation seems to be linked ~~with~~ to the intensified Kuroshio Current since 8.5 ka. The enhanced formation of NPIW during HS1 can be driven by the perturbation of sea ice formation and sea surface salinity oscillation in high-latitude North Pacific. ~~The~~ In our results, ~~de~~ diminished sedimentary oxygenation during the B/A due to upwelling of aged, nutrient-rich deep water and enhanced export production, indicates an enhanced CO₂ sequestration at mid-depth waters, along with a slight increase in atmospheric ~~CO₂~~ concentration. ~~Mechanistically, we~~ We speculate that ~~attribute~~ these millennial-scale

带格式的: 无下划线, 字体颜色: 自动设置

64 changes ~~were linked to the intensified NPIW and enhanced abyss flushing during~~
65 ~~deglacial cold and warm intervals, respectively, on the basis of background climate~~
66 ~~change due to shift in strength of North Atlantic Deep Water formation, leading to~~
67 ~~intensification of NPIW formation and enhanced abyss flushing during deglacial cold~~
68 ~~and warm intervals, respectively. Enhanced formation of NPIW seem to be driven by~~
69 ~~the perturbation of sea ice formation and sea surface salinity oscillation in high~~
70 ~~latitude North Pacific through atmospheric and oceanic teleconnection. During the~~
71 ~~B/A, decreased sedimentary oxygenation likely resulted from an upward penetration~~
72 ~~of aged deep water into the intermediate depth in the North Pacific, corresponding to~~
73 ~~a resumption of Atlantic Meridional Overturning Circulation.~~

带格式的: 无下划线, 字体颜色: 自动设置

带格式的: 无下划线, 字体颜色: 自动设置

74 **Keywords:** ~~sedimentary oxygenation; millennial timescale; North Pacific~~
75 ~~Intermediate Water; North Atlantic Deep Water Atlantic Meridional Overturning~~
76 ~~Circulation; subtropical North Pacific~~

带格式的: 无下划线, 字体颜色: 自动设置

带格式的: 首行缩进: 0 字符, 行距: 1.5 倍行距

带格式的: 缩进: 首行缩进: 0 字符, 行距: 1.5 倍行距

1. Introduction

The sluggish ocean ventilation and efficient biological pump in the ocean ~~depletes dissolved oxygen in the sediment water interface and~~ facilitates the carbon storage-sequestration of respired in the ocean interior-carbon, linking to atmospheric CO₂ drawdown, which in turn plays a crucial role in regulating sedimentary oxygen; ~~potentially linking to atmospheric CO₂ changes~~ on millennial and orbital ~~and millennial~~ timescales (Hoogakker et al., 2015; Jaccard and Galbraith, 2012; Sigman and Boyle, 2000). ~~The r~~Reconstruction of past sedimentary oxygenation is therefore crucial for understanding changes in export productivity and the renewal rate of deep ocean circulation (Nameroff et al., 2004). Previous studies from high-latitude eastern and western North Pacific margins~~s~~ and subarctic Pacific have identified drastic variations in export productivity and marine-ocean oxygen levels at glacial-interglacial timescales using diverse proxies such as trace elements (Cartapanis et al., 2011; Chang et al., 2014; Jaccard et al., 2009; Zou et al., 2012), benthic foraminiferal assemblages (Ohkushi et al., 2016; Ohkushi et al., 2013; Shibahara et al., 2007) and nitrogen isotopic composition ($\delta^{15}\text{N}$) of organic matter (Addison et al., 2012; Chang et al., 2014; Galbraith et al., 2004; Riethdorf et al., 2016) in marine sediment ~~cored sediments~~. These studies further suggested that both North Pacific Intermediate Water (NPIW) and export of organic carbon-matter regulate the sedimentary oxygenation variation during the last glaciation and Holocene in the northeast-subarctic North Pacific. By contrast, little information exists on millennial-scale oxygenation changes to date in the western subtropical North Pacific.

The modern NPIW is mainly sourced from the NW Pacific marginal seas (Shcherbina et al., 2003; Talley, 1993; You et al., 2000), and then it spreads into subtropical North Pacific at intermediate depths of 300 to 800 m (Talley, 1993). The pathway and circulation of NPIW have been identified by You (2003), who suggested that cabbelling, a mixing process to form a new water mass with increased density than that of parent water masses, is the principle mechanism responsible for transforming subpolar source waters into subtropical NPIW along the subarctic-tropical frontal zone. More specifically, You et al. (2003) argued that a

带格式的: 无下划线, 字体颜色: 自动设置

109 lower subpolar input of about 2 Sv ($1 \text{ Sv} = 10^6 \text{ m}^3/\text{s}$) is sufficient for subtropical
110 ventilation. Benthic foraminiferal $\delta^{13}\text{C}$ -~~data, a quasi-conservative tracer for water~~
111 ~~mass,~~ from the North Pacific suggested an enhanced ventilation (enriched $\delta^{13}\text{C}$) at
112 water depths of < 2000 m during the last glacial period (Keigwin, 1998; Matsumoto et
113 al., 2002). Furthermore, on the basis of both radiocarbon data and modeling results,
114 Okazaki et al. (2010) provided further insight into the formation of deep water in the
115 North Pacific during early deglaciation. Enhanced NPIW penetration is further
116 explored using numerical model simulations (Chikamoto et al., 2012; Gong et al.,
117 2019; Okazaki et al., 2010). ~~The downstream effects of intensified GNPIW can be~~
118 ~~seen in the record of $\delta^{13}\text{C}$ of *Cibicides wuellerstorfi* in core PN-3 from the middle~~
119 ~~Okinawa Trough (OT), whereas lower deglacial $\delta^{13}\text{C}$ values were attributed to~~
120 ~~enhanced OC accumulation rates due to higher surface productivity by Wahyudi and~~
121 ~~Minagawa (1997). More recently, Max et al (2017) identified the substantial effects of~~
122 ~~intensified NPIW on $\delta^{13}\text{C}$ of deep-dwelling planktic foraminifera *Globorotaloides*~~
123 ~~*hexagonus* in the Eastern Equatorial Pacific during Marine Isotope Stage (MIS) 2.~~
124 ~~Subsequently, Rippert et al. (2017) confirmed that such enhanced effect of NPIW also~~
125 ~~occurred during MIS 6. The downstream effects of intensified NPIW also can be seen~~
126 ~~in the record of $\delta^{13}\text{C}$ of *Cibicides wuellerstorfi* in core PN-3 from the middle~~
127 ~~Okinawa Trough (OT), whereas lower deglacial $\delta^{13}\text{C}$ values were attributed to~~
128 ~~enhanced OC accumulation rates due to higher surface productivity by Wahyudi and~~
129 ~~Minagawa (1997).~~
130 The Okinawa Trough is separated from the Philippine Sea by the Ryukyu Islands
131 and is an important channel of the northern extension of the Kuroshio in the western
132 subtropical North Pacific (Figure 1). Initially the OT opened at the middle Miocene
133 (Sibuet et al., 1987) and since then, it has been a depositional center in the East China
134 Sea (ECS), receiving large sediment supplies from nearby rivers (Chang et al., 2009).
135 Surface hydrographic characteristics of the OT over glacial-interglacial cycles are
136 largely influenced by the Kuroshio and ~~East China Sea~~ECS Coastal Water (Shi et al.,
137 2014); the latter is related to the strength of summer East Asian monsoon (EAM)
138 sourced from the western tropical Pacific. Modern physical oceanographic

带格式的: 无下划线, 字体颜色: 自动设置

139 investigations showed that intermediate waters in the OT are mainly derived from
140 horizontal advection and mixture of NPIW and South China Sea Intermediate Water
141 (Nakamura et al., 2013). These waters intrude into the OT through two ways
142 (Nakamura et al., 2013): (i) deeper part of the Kuroshio enters the OT through the
143 channel east of Taiwan (sill depth 775 m) and (ii) through the Kerama Gap (sill depth
144 1100 m). In the northern OT, the occupied subsurface water mainly flows through the
145 Kerama Gap through horizontal advection from the Philippine Sea (Nakamura et al.,
146 2013). Recently, Nishina et al. (2016) found that an overflow through the Kerama Gap
147 controls the modern deep-water ventilation in the southern OT.

148 Both surface hydrography and deep ventilation in the OT varied greatly since the
149 last glaciation. During the last glacial periods, the mainstream of the Kuroshio likely
150 migrated to the east of the Ryukyu Islands or and also became weaker due to lower
151 sea levels (Shi et al., 2014; Ujiie and Ujiie, 1999; Ujiie et al., 2003) and the
152 hypothetical emergence of a Ryukyu-Taiwan land bridge (Ujiie and Ujiie, 1999). In a
153 recent study, based on the Mg/Ca-derived temperatures in surface and thermocline
154 waters and planktic foraminiferal indicators of water masses from two sediment cores
155 located in the northern and southern OT, Ujiie et al. (2016) further argued that the
156 hydrological conditions of North Pacific Subtropical Gyre since MIS 7 is modulated
157 by the interaction between the Kuroshio and the NPIW. Besides the Kuroshio, the
158 flux of East Asian rivers to the East China Sea (ECS), which is related to the summer
159 EAM and the sea level oscillations coupled with topography are also have also been
160 regulating the surface hydrography in the Okinawa Trough OT (Chang et al., 2009;
161 Kubota et al., 2010; Sun et al., 2005; Yu et al., 2009).

162 Based on benthic foraminiferal assemblages, previous studies have implied a
163 reduced oxygenation in deep waters of the middle and southern OT during the last
164 deglacial period (Jian et al., 1996; Li et al., 2005), but a strong ventilation during the
165 Last Glacial Maximum (LGM) and the Holocene (Jian et al., 1996; Kao et al., 2005).
166 High sedimentary $\delta^{15}\text{N}$ values, an indicator of increased denitrification in the
167 subsurface water column, also occurred during the late deglaciation in the middle OT
168 (Kao et al., 2008). Inconsistent with these results, Dou et al. (2015) suggested an oxic

带格式的: 无下划线, 字体颜色: 自动设置

169 depositional environment during the last deglaciation in the southern OT based on
170 weak positive cerium anomalies. Furthermore, Kao et al. (2006) concluded a reduced
171 ventilation of deepwater in the OT during the LGM due to the reduction of KC inflow
172 using a 3-D ocean model. Yet, the patterns and reasons that caused sedimentary
173 oxygenation in the OT thus remain unclear.

带格式的: 无下划线, 字体颜色: 自动设置

带格式的: 无下划线, 字体颜色: 自动设置

174 2. Paleo-redox proxies

带格式的: 无下划线, 字体颜色: 自动设置

带格式的: 无下划线, 字体颜色: 自动设置

175 Sedimentary redox condition is ~~the balance between~~governed by the rate of
176 oxygen supply from the overlying bottom water and the rate of oxygen removal from
177 pore water (Jaccard et al., 2016), processes that are ~~closely~~ related to the ~~supply of~~
178 ~~oxygen by ocean circulation~~advection of submarine ocean circulation and organic
179 matter respiration, respectively. Contrasting geochemical behaviors of redox-sensitive
180 trace metals (Mn, Mo, U, etc.) have been ~~extensively~~ used to reconstruct bottom water
181 and sedimentary oxygen changes (Algeo, 2004; Algeo and Lyons, 2006; Crusius et al.,
182 1996; Dean et al., 1997; Tribovillard et al., 2006; Zou et al., 2012), as their
183 concentrations ~~readily~~ respond to redox condition of the depositional environment
184 (Morford and Emerson, 1999).

带格式的: 无下划线, 字体颜色: 自动设置

带格式的: 无下划线, 字体颜色: 自动设置

带格式的: 无下划线, 字体颜色: 自动设置

带格式的: 无下划线, 字体颜色: 自动设置

185 In general, enrichment of Mn with higher speciation states (Mn (III) and Mn (IV))
186 in the form of Mn-oxide coatings is observed in marine sediments, when oxic
187 condition prevails into ~~greater~~ sediment depths as a result of low organic matter
188 degradation rates and well-ventilated bottom water (Burdige, 1993). ~~In-Under~~
189 reducing conditions, ~~the authigenic fraction of Mn~~ (as opposed to its detrital
190 ~~background~~) is released as dissolved Mn (II) species into the pore water and thus its
191 concentration is usually low in suboxic (O₂ and HS⁻ absent) and anoxic (HS⁻ present)
192 sediments. In addition, when Mn enrichment occurs in oxic sediments as solid phase
193 Mn oxyhydroxides, it may lead to co-precipitation of other elements, such as Mo
194 (Nameroff et al., 2002).

带格式的: 无下划线, 字体颜色: 自动设置

195 The elements Mo and U behave conservatively in oxygenated seawater, but are
196 preferentially enriched in oxygen-depleted water (Morford and Emerson, 1999).

带格式的: 无下划线, 字体颜色: 自动设置

带格式的: 无下划线, 字体颜色: 自动设置

域代码已更改

197 However, these two trace metals behave differently in several ways. Molybdenum can
198 be enriched in both oxic sediments, such as the near surface manganese-rich horizons

199 in continental margin environments (Shimmield and Price, 1986) and in anoxic
200 sediments (Nameroff et al., 2002). Under anoxic conditions, Mo can be reduced either
201 from the +6 oxidation state to insoluble MoS₂, though this process is known to occur
202 only under extremely reducing conditions, such as hydrothermal and/or diagenesis
203 (Dahl et al., 2010; Helz et al., 1996) or be converted to particle-reactive
204 thiomolybdates (Vorlicek and Helz, 2002). Zheng et al. (2000) suggested two critical
205 thresholds for Mo scavenging from seawater: 0.1 μM hydrogen sulfide (H₂S) for
206 Fe-S-Mo co-precipitation and 100 μM H₂S for Mo scavenging as Mo-S or as
207 particle-bound Mo without Fe. Although Crusius et al. (1996) noted insignificant
208 enrichment of sedimentary Mo under suboxic conditions, Scott et al. (2008) argued
209 that burial flux of Mo is not so low in suboxic environments. Excess concentration of
210 Mo (Mo_{excess}) in sediments thus suggests the accumulation of sediments either in
211 anoxic (H₂S occurrence) or well oxygenated conditions (if Mo_{excess} is in association
212 with Mn-oxides).

213 In general, U is enriched in anoxic sediments (>1 μM H₂S), but not in oxic
214 sediments (>10 μM O₂) (Nameroff et al., 2002). Accumulation of U depends on the
215 content of reactive organic matter (Sundby et al., 2004) and U precipitates as uraninite
216 (UO₂) during the conversion of Fe (III) to Fe (II) in suboxic conditions (Morford and
217 Emerson, 1999; Zheng et al., 2002). One of the primary removal mechanisms for U
218 from the ocean is via diffusion across the sediment-water interface of reducing
219 sediments (Klinkhammer and Palmer, 1991). Under suboxic conditions, soluble U (VI)
220 is reduced to insoluble U (IV), but free sulfide is not required for U precipitation
221 (McManus et al., 2005). Jaccard et al. (2009) suggested that the presence of excess
222 concentration of U (U_{excess}) in the absence of Mo enrichment is indicative of a suboxic,
223 but not sulfidic condition, within the diffusional range of the sediment-water interface.
224 The felsic ~~volcanic~~ volcanism is also a primary source of uranium (Maithani and
225 Srinivasan, 2011). Therefore, the potential input of uranium from active volcanic
226 sources around the northwestern Pacific to the adjacent sediments should not be
227 neglected.

228 In this study, we investigate a suite of redox-sensitive elements and the ratio of

域代码已更改

229 Mo/Mn along with productivity proxies from a sediment core retrieved from the
230 northern OT to reconstruct the sedimentary oxygenation in the western subtropical
231 North Pacific over the last 50ka. Based on that, we propose that multiple factors, such
232 as NPIW ventilation, the strength of the Kuroshio Current and export productivity,
233 control the bottom sedimentary oxygenation in the OT on millennial time-scales since
234 the last glacial.

235 3. Oceanographic setting

236 ~~The OT resulted from the collision of the Philippine and Eurasian plates and~~
237 ~~initially opened at the middle Miocene (Sibuet et al., 1987). Since that time, the OT~~
238 ~~has been a depositional center in the ECS and receives large sediment supplies from~~
239 ~~nearby rivers (Chang et al., 2009). At present, water depth in the axial part of the OT~~
240 ~~deepens from 500 m in the north to 2700 m in the south.~~

241 Surface hydrographic characteristics of the OT are mainly controlled by the
242 warmer, more saline, oligotrophic Kuroshio water and cooler, less saline, nutrient-rich
243 Changjiang Diluted Water, and the modern flow-path of the former is influenced by
244 the bathymetry of the OT (Figure 1a). The Kuroshio Current originates from the
245 North Equatorial Current and flows into the ECS from the Philippine Sea through the
246 Suao-Yonaguni Depression. In the northern OT, Tsushima Warm Current (TWC), a
247 branch of the Kuroshio, flows into the Japan Sea through the shallow Tsushima Strait.
248 Volume transport of the Kuroshio varies seasonally due to the influence of the EAM
249 with a maximum of 24 Sv ($1\text{ Sv} = 10^6\text{ m}^3/\text{s}$) in summer and a minimum of 20 Sv in
250 autumn across the east of Taiwan (Qu and Lukas, 2003).

251 Figures 2a and 2b and b show that the lower sea surface salinity (SSS) zone in
252 summer relative to the one in winter in the ECS migrates toward the east of OT,
253 indicating enhanced impact of the Changjiang discharge associated with summer
254 EAM. An estimated ~80% of The-the mean annual discharge of ~~the~~ Changjiang ~~is~~
255 0.028 Sv and ~80% of its total discharge is supplied to the ECS (Ichikawa and
256 Beardsley, 2002). ~~In and in situ observational data of surface hydrography along the~~
257 ~~ship track from Taiwan Strait to Korea Strait and around the entrance of the Tsushima~~
258 ~~Strait in the northern part of the ECS show a lower SSS in summer and a pronounced~~

域代码已更改

域代码已更改

域代码已更改

域代码已更改

带格式的：字体：(中文)+中文正文，
小四，非突出显示

带格式的：字体：小四，非突出显示

域代码已更改

域代码已更改

259 negative correlation between the Changjiang discharge and SSS in July (Delcroix and
260 Murtugudde, 2002). ~~Lower SSS in summer than that in winter suggests stronger~~
261 ~~effects of summer EAM on surface hydrography over the Kuroshio Current (Sun et al.,~~
262 ~~2005).~~ Consistently, previous studies from the Okinawa Trough reported such
263 close relationship between summer EAM and SSS back to the late Pleistocene (Chang
264 et al., 2009; Clemens et al., 2018; Kubota et al., 2010; Sun et al., 2005).

265 Despite the effects of EAM and the Kuroshio, evidence of geochemical tracers
266 (temperature, salinity, oxygen, nutrients and radiocarbon- $\Delta^{14}\text{C}$) collected during the
267 World Ocean Circulation Experiment (WOCE) Expeditions in the Pacific (transects
268 P24 and P03) favors the presence of low saline, nutrient-enriched intermediate and
269 deep waters (Talley, 2007). Dissolved oxygen content is $<100 \mu\text{M}/\text{mol}/\text{kg}$ at water
270 depths of below 600 m in the OT along WOCE transects PC03 and PC24 (Talley,
271 2007). Modern oceanographic observations at the Kerama Gap reveal that upwelling
272 in the OT is associated with the inflow of NPIW and studies using box model
273 predicted that overflow through the Kerama Gap is responsible for upwelling ($3.8\text{--}7.6$
274 $\times 10^{-6} \text{m s}^{-1}$) (Nakamura et al., 2013; Nishina et al., 2016).

275 4. Materials and methods

276 4.1. Chronostratigraphy of core CSH1

277 A 17.3 m long sediment core CSH1 ($31^{\circ} 13.7' \text{N}$, $128^{\circ} 43.4' \text{E}$; water depth: 703
278 m) was collected from the northern OT, close to the main stream of Tsushima Warm
279 Current (TWC) (Figure 1b) and within the depth of NPIW (Figure 1c) using a piston
280 corer during *Xiangyanghong09* Cruise in 1998. This location is thus enabling us to
281 reconstruct millennial-scale changes in the properties of TWC and NPIW. The
282 expedition was carried out by the First Institute of Oceanography, Ministry of Natural
283 Resources of China. Core CSH1 mainly consists of clayey silt and silt with
284 occurrence of plant debris at some depth intervals (Ge et al., 2007) (Figure 3a). In
285 addition, three layers of volcanic ash were observed at depths of 74–106 cm, 782–794
286 cm, 1570–1602 cm and these three intervals can be correlated with well-known ash
287 layers, Kikai-Akahoya (K-Ah; 7.3 ka), Aira-Tanzawa (AT; 29.24 ka) and Aso-4
288 (roughly around MIS 5a) (Machida, 1999), respectively. The core was split and

域代码已更改

域代码已更改

域代码已更改

域代码已更改

域代码已更改

域代码已更改

域代码已更改

域代码已更改

域代码已更改

289 sub-sampled at every 4 cm interval and then stored in China Ocean Sample
290 Repository at 4 °C until analysis.

291 Previously, some paleoceanographic studies have been conducted and a set of
292 data have been investigated for core CSH1, including the contents of planktic
293 foraminifers as well as their carbon ($\delta^{13}\text{C}$) and oxygen isotope ($\delta^{18}\text{O}$) compositions
294 (Shi et al., 2014), pollen (Chen et al., 2006), paleomagnetism (Ge et al., 2007) and
295 CaCO_3 (Wu et al., 2004). An age model for this core has been constructed by using
296 ten Accelerator Mass Spectrometry (AMS) ^{14}C dates and six oxygen isotope ($\delta^{18}\text{O}$)
297 age control points. The whole 17.3 m core contains *ca.* 88 ka-long record of
298 continuous sedimentation (Shi et al., 2014).

299 It is noteworthy that previous age control points with constant radiocarbon
300 reservoir throughout core CSH1 are used to reveal orbital-scale Kuroshio variations
301 (Shi et al., 2014), but insufficient to investigate millennial-scale climatic events. On
302 the basis of original age model, a higher abundance of *Neogloboquadrina*
303 *pachyderma* (*dextral*) that occurred during warmer intervals, such as the B/A, has
304 been challenging to explain reasonably. On the other hand, paired measurements of
305 $^{14}\text{C}/^{12}\text{C}$ and ^{230}Th ages from Hulu Cave stalagmites suggest magnetic field change has
306 greatly contributed to high atmospheric $^{14}\text{C}/^{12}\text{C}$ values at HS4 and the YD (Cheng et
307 al., 2018). Thus a constant reservoir age assumed when calibrating foraminiferal
308 radiocarbon dates using CALIB 6 software and the Marine_13 calibration dataset
309 (Reimer et al., 2013) for ~~Core-core~~ CSH1 may cause large chronological
310 uncertainties.

311 Here, we therefore recalibrated the radiocarbon dates using CALIB 7.04 software
312 with Marine 13 calibration dataset (Reimer et al., 2013). Moreover, on the basis of
313 significant correlation between planktic foraminiferal species *Globigerinoides ruber*
314 $\delta^{18}\text{O}$ and Chinese stalagmite $\delta^{18}\text{O}$ (Cheng et al., 2016), a proxy of summer EAM
315 related to SSS of the ECS, we re-established the age model for core CSH1 (Figures
316 3b-d). Overall, the new chronological framework is similar to the one previously
317 reported by Shi et al. (2014), but with more dates. In order to compare with published
318 results associated with ventilation changes in the North Pacific, here we mainly report

域代码已更改

319 | the history of sedimentary oxygenation in the northern OT since the last glacial period.
320 | Linear sedimentation rate varied between ~ 10 and ~~60–40~~ cm/ka with higher
321 | sedimentation rate (around 30–40 cm/ka) between ~ 24 ka and 32.5 ka. The age control
322 | points were shown in Table 2.–

323 | **4.2. Chemical analyses**

324 | Sediment subsamples for geochemical analyses were freeze-dried and ground to
325 | a fine powder with an agate mortar and pestle. Based on the age model, 85
326 | subsamples from core CSH1 with time resolution of about ~~200–600~~ years (every 4 cm
327 | interval) were selected for detailed geochemical analyses of major and minor
328 | elements and total contents of carbon (TC), organic carbon (TOC) and nitrogen (TN).
329 | The pretreatment of sediment and other analytical methods have been reported
330 | elsewhere (Zou et al., 2012).

331 | TC and TN were determined with an elemental analyzer (EA; Vario EL III,
332 | Elementar Analysen systeme GmbH) in the Key Laboratory of Marine Sediment and
333 | Environment Geology, First Institute of Oceanography, Ministry of Natural Resources
334 | of China, Qingdao. Carbonate was removed from sediments by adding 1M HCl to the
335 | homogenized sediments for total organic carbon (TOC) analysis using the same
336 | equipment. The content of calcium carbonate (CaCO_3) was calculated using the
337 | equation:

$$338 | \text{CaCO}_3 = (\text{TC} - \text{TOC}) \times 8.33$$

339 | where 8.33 is the ratio between the molecular weight of carbonate and the atomic
340 | weight of carbon. National reference material (GSD-9), blank sample and replicated
341 | samples were used to control the analytical process. The relative standard deviation of
342 | the GSD-9 for TC, TN and TOC is $\leq 3.4\%$.

343 | About 0.5 g of sediment powder was digested in double distilled $\text{HF}:\text{HNO}_3$ (3:1),
344 | followed by concentrated HClO_4 , and then re-dissolved in 5% HNO_3 . Selected major
345 | and minor elements such as aluminum (Al) and manganese (Mn) were determined by
346 | inductively coupled plasma optical emission spectroscopy (ICP-OES; Thermo
347 | Scientific iCAP 6000, Thermo Fisher Scientific), as detailed elsewhere (Zou et al.,
348 | 2012). In addition, Mo and U were analyzed with inductively coupled plasma mass

域代码已更改

域代码已更改

349 spectrometry (ICP-MS; Thermo Scientific XSERIES 2, Thermo Fisher Scientific), as
350 described in Zou et al. (2012). Precision for most elements in the reference material
351 GSD-9 is $\leq 5\%$ relative standard deviation. The excess fractions of U and Mo were
352 estimated by normalization to Al:

353
$$\text{Excess fraction} = \frac{\text{total}_{\text{element}} - (\text{element}/\text{Al}_{\text{average shale}} \times \text{Al})}{\text{Al}_{\text{average shale}}}$$
, with $\text{U}/\text{Al}_{\text{average shale}} =$
354 0.307×10^{-6} and $\text{Mo}/\text{Al}_{\text{average shale}} = 0.295 \times 10^{-6}$ (Li and Schoonmaker, 2014).

355 In addition, given the different geochemical behaviors of Mn and Mo and
356 co-precipitation and adsorption processes associated with the redox cycling of Mn, we
357 calculated the ratio of Mo to Mn, ~~given assuming~~ that higher Mo/Mn ratio indicates
358 lower oxygen content in the depositional environment and vice versa. In combination
359 with the concentration of excess uranium, we infer the history of sedimentary
360 oxygenation in the subtropical North Pacific since the last glaciation.

361 5. Results

362 5.1. TOC, TN, and CaCO₃

363 The content of CaCO₃ varies from 8.8 to 35% (Figure 4a) and it mostly shows
364 higher values with increasing trends during the last deglaciation. In contrast, the
365 content of CaCO₃ is low and exhibits decreasing trends during the late MIS 3 and the
366 LGM (Figure 4a). TN content shows a larger variation compared to TOC (Figure 4b),
367 but it still strongly correlates with TOC ($r = 0.74$, $p < 0.01$) throughout the entire core.
368 Concentration of TOC ranges from 0.5 to 2.1% and it shows higher values with stable
369 trends during the last glacial phase (MIS 3) (Figure 4c). Molar ratios of TOC/TN vary
370 around 10, with higher ratios at the transition into the LGM (Figure 4d),
371 corresponding to higher linear sedimentation rate (Figure 4a4e). ~~The content of~~
372 ~~CaCO₃ varies from 8.8 to 35% (Figure 4e) and it mostly shows higher values with~~
373 ~~increasing trends during the last deglaciation. Conversely, the content of CaCO₃ is low~~
374 ~~and exhibits decreasing trends during late MIS 3 and the LGM (Figure 4e).~~

375 Both TOC and CaCO₃ have been ~~are widely~~ used as proxies for the
376 reconstruction of past export productivity (Cartapanis et al., 2011; Lembke-Jene et al.,
377 2017; Rühlemann et al., 1999). Molar C/N ratios of >10 (Figure 4c) suggest that
378 terrigenous organic sources significantly contribute to the TOC concentration in core

域代码已更改

带格式的: 字体: Times New Roman

域代码已更改

域代码已更改

379 CSH1. The TOC content therefore may be not a reliable proxy for the reconstruction
380 of surface water export productivity during times of the LGM and late deglaciation,
381 when maxima in C/N ratios co-occur with decoupled trends between CaCO₃ and TOC
382 concentrations.

383 ~~Several lines of evidence support CaCO₃ as a reliable productivity proxy,~~
384 ~~particularly during the last deglaciation. (Shi et al., 2014)In addition, †The strong~~
385 negative correlation coefficient ($r = -0.85$, $p < 0.01$) between Al and CaCO₃ in
386 sediments throughout core CSH1 confirms the biogenic origin of CaCO₃ against
387 terrigenous Al (Figure 4f). ~~Generally, terrigenous dilution decreases the~~
388 ~~concentrations of CaCO₃. Inconsistent relationship between percentage CaCO₃ and~~
389 ~~sedimentation rate indicates a minor effect of dilution on CaCO₃. Furthermore, the~~
390 ~~increasing trend in CaCO₃ associated with high sedimentation rate during the last~~
391 ~~deglacial interval indicates a substantial increase in export productivity (Figures 4a~~
392 ~~and 4d). The high coherence between percentage CaCO₃ and alkenone-derived sea~~
393 ~~surface water (SST) (Shi et al., 2014) indicates a direct control on CaCO₃ by SST.~~
394 Moreover, a detailed comparison between CaCO₃ concentrations and the previously
395 published foraminiferal fragmentation ratio (Wu et al., 2004) ~~clearly~~ shows, apart
396 from a small portion within the LGM, no clear co-variation ~~between them. This-These~~
397 ~~evidence~~ suggests that CaCO₃ changes are ~~primarily~~ driven ~~primarily~~ by variations in
398 carbonate primary production, and not overprinted by secondary processes, such as
399 carbonate dissolution ~~through changes in the lysocline depth— and dilution by~~
400 ~~terrigenous materialsthrough changes in the lysocline depth. Likewise, similar~~
401 ~~deglacial trend in CaCO₃ is also observed in core MD01-2404 (Chang et al., 2009),~~
402 ~~indicating a ubiquitous, not local picture in the OT. On the other hand, terrigenous~~
403 ~~dilution generally decreases the content of CaCO₃.—All these lines of evidence thus~~
404 ~~support CaCO₃ of core CSH1 as a reliable productivity proxy to a first order~~
405 ~~approximation. The increasing trend of CaCO₃ associated with high sedimentation rate~~
406 ~~(Figures 4a, e) indicates a substantial increase in export productivity during the last~~
407 ~~deglacial interval. Thus, we can confidently use CaCO₃ content as productivity proxy~~
408 ~~to a first order approximation.~~

域代码已更改

域代码已更改

带格式的：下标

带格式的：下标

域代码已更改

域代码已更改

域代码已更改

409 5.2. Redox-sensitive Elements

410 Figure 4 shows time series of selected redox-sensitive elements (RSEs) and
411 proxies derived from them. Mn shows higher concentrations during the LGM and
412 HS1 (16 ka–22.5 ka) and middle-late Holocene, but lower concentrations during the
413 last deglacial and Preboreal periods (15.8 ka–9.5 ka) (Figure 4g). Generally,
414 concentrations of excess Mo and excess U (Figures 4j and, 4l) show coherent patterns
415 with those of Mo and U (Figures 4i and, 4k), but both are out-of-phase with Mn over
416 the last glacial period (Figure 4h). It should be noted that pronounced variations in U
417 concentration since 8.5 ka is related to the occurrence of discrete volcanic materials.

418 A significant positive Eu anomaly (Zhu et al., 2015) (Zhu et al., 2015) together with
419 more radiogenic Nd values (unpublished data) from the same core confirms the
420 occurrence of discrete volcanic materials and its dilution effects on terrigenous
421 components since 7 ka. Occurrence of discrete volcanic material is likely related to
422 intensified Kuroshio Current during the mid-late Holocene, as supported by higher
423 hydrothermal Hg concentrations in sediments from the middle OT (Lim et al., 2017).

424 A negative correlation between Mn and Mo_{excess} during the last glaciation and the
425 Holocene, and the strong positive correlation between them during the LGM and HS1
426 (Figures 5a and 5b) further corroborate the complicated geochemical behaviors of Mn
427 and Mo. A strong positive correlation between Mo_{excess} and Mn (Figure 5b) seems
428 to may be attributed to co-precipitation of Mo by Mn-oxyhydroxide under oxygenated
429 conditions. Here, we use Mo/Mn ratio, instead of excess Mo concentration to
430 reconstruct variations in sedimentary redox state conditions in the study area. Overall,
431 the Mo/Mn ratio shows similar downcore pattern to that of Mo_{excess} with higher values
432 ratios during the last deglaciation, but lower values-ratios during the LGM and HS1. A
433 strong correlation (r = 0.69) between Mo/Mn ratio and excess U concentration
434 (excluding the data of Holocene, due to contamination of volcanic material, Figure 5c)
435 further corroborates the integrity of Mo/Mn as an indicator of sedimentary
436 oxygenation changes.

437 Rapidly decreasing Mo/Mn ratio indicates an oxygenated sedimentary
438 environment since ~8 ka (Figure 4h). Both higher Mo/Mn ratios and excess U

域代码已更改

域代码已更改

域代码已更改

域代码已更改

439 concentration, together with lower Mn concentrations suggest an ~~oxygen-deficient~~
440 ~~deoxygenated sedimentary-depositional condition environment~~ during the late
441 deglacial period (15.8 ~~ka~~-9.5 ka), whereas lower ~~values-ratios~~ during the LGM, HS1
442 and HS2 indicate relatively better oxygenated sedimentary condition. A decreasing
443 trend in Mo/Mn ratio and excess U concentration from 50 ka to 25 ka also suggest
444 higher sedimentary oxygen levels.

445 6. Discussion

446 6.1. Constraining paleoredox conditions in the Okinawa Trough

447 In general, three different terms, hypoxia, suboxia and anoxia, are widely used to
448 describe the degree of oxygen depletion in the marine environment (Hofmann et al.,
449 2011). ~~Here, we adopt the definition of oxygen thresholds by Bianchi et al. (2012), for~~
450 ~~oxic (>120 $\mu\text{mol/kg O}_2$), hypoxic (<60-120 $\mu\text{mol/kg O}_2$) and suboxic (<2-10~~
451 ~~$\mu\text{mol/kg O}_2$) conditions, whereas anoxia is the absence of measurable~~
452 ~~oxygen. Generally, redox states in waters can be classified as oxic (>89 $\mu\text{mol/L O}_2$),~~
453 ~~suboxic (<8.9-89 $\mu\text{mol/L O}_2$), anoxic-nonsulfidic (<89 $\mu\text{mol/L O}_2$, 0 $\mu\text{mol/L H}_2\text{S}$),~~
454 ~~and anoxic-sulfidic or euxinic (0 $\text{ml O}_2/\text{L}$, >0 $\mu\text{mol/L H}_2\text{S}$) (Savrda and Bottjer,~~
455 ~~1991).~~

456 Proxies associated with RSEs, such as sedimentary Mo concentration (Lyons et
457 al., 2009; Scott et al., 2008) have been used to constrain the degree of oxygenation in
458 seawater. Algeo and Tribouillard (2009) proposed that open-ocean systems with
459 suboxic waters tend to yield U_{excess} enrichment relative to Mo_{excess} ~~a, nd to~~
460 ~~resultresulting~~ in sediment $(Mo/U)_{\text{excess}}$ ratio less than that of seawater (7.5-7.9).
461 Under increasingly reducing and occasionally sulfidic conditions, the accumulation of
462 Mo_{excess} increase relative to that of U_{excess} leading the $(Mo/U)_{\text{excess}}$ ratio either is equal
463 to or exceeds with that of seawater. Furthermore, Scott and Lyons (2012) suggested a
464 non-euxinic condition with the presence of sulfide in pore waters, when Mo
465 concentrations range from > 2 ~~ppm $\mu\text{g/g}$~~ , the crustal average to < 25 ~~ppm $\mu\text{g/g}$~~ , a
466 threshold concentration for euxinic condition. Given that the ~~northern~~Okinawa Trough
467 ~~OT~~ is located in ~~the open oceanic settings~~~~weakly restricted basin settings~~, we use
468 these two above mentioned proxies to evaluate the degree of oxygenation in

带格式的：字体：(中文) 宋体

带格式的：字体：(中文) 宋体

带格式的：字体：(中文) 宋体

带格式的：字体：(中文) 宋体，下标

带格式的：字体：(中文) 宋体

带格式的：字体：(中文) 宋体，下标

带格式的：字体：(中文) 宋体

带格式的：字体：(中文) 宋体，下标

带格式的：字体：(中文) 宋体

带格式的：字体：(中文) 宋体

带格式的：字体：(中文) 宋体

带格式的：字体：(中文) 宋体

带格式的：字体：(中文) 宋体

带格式的：字体：(中文) 宋体

域代码已更改

域代码已更改

域代码已更改

带格式的：字体：小四

带格式的：字体：小四

469 sediments.

470 Both bulk Mo concentration (1.2-9.5 ppm μ g/g) and excess (Mo/U) ratio (0.2-5.7)
471 in core CSH1 suggest that oxygen-depleted conditions may have prevailed in the deep
472 water of the northern OT over the last 50 ka (Figure 4m). However, increased excess
473 Mo concentration with enhanced Mo/U ratio during the last termination (18-9 ka)
474 indicate a stronger reducing condition compared to the Holocene and the last glacial
475 period, though Mo concentration is less than 25 ppm μ g/g, a threshold for euxinic
476 deposition proposed by Scott and Lyons (2012).

477 The relative abundance of benthic foraminiferal species that thrive in different
478 oxygen concentrations also have been widely used to reconstruct the variations in
479 bottom water ventilation, such as enhanced abundance of *Bulimina aculeata*,
480 *Uvigerina peregrina* and *Chilostomella oolina* found under oxygen-depleted
481 conditions in the central and southern OT during the last deglaciation (18 ka -9.2 ka)
482 (Jian et al., 1996; Li et al., 2005). An oxygenated bottom water condition is also
483 indicated by abundant benthic foraminifera species *Cibicides hyalina* and
484 *Globocassidulina subglobosa* after 9.2 ka (Jian et al., 1996; Li et al., 2005) in cores
485 E017 (1826 m water depth), 255 (1575 m water depth) and high benthic $\delta^{13}\text{C}$ values
486 (Wahyudi and Minagawa, 1997) in cores E017 (water depth 1826 m), 225 (water
487 depth 1575 m) in core and PN-3 (water depth 1058 m water depth) from the middle
488 and southern OT (Figures 1 and 3) during the postglacial period. The inferred
489 ventilation pattern poorly-ventilated deep water in the middle and southern OT
490 inferred from by benthic foraminiferal assemblages during the last deglaciation is
491 coeval consistent with the one inferred from RSEs in this northern OT study referring
492 to our RSEs (Figure 4). A clear linkage thus can be established between deep-water
493 ventilation and sedimentary oxygenation in the OT. Although we did not carry out
494 benthic foraminiferal species analyses for our core CSH1, it is reasonable to infer
495 based on RSEs that the deepwater in the northern OT was also in a prominent
496 oxygen-poor condition during the late deglacial interval. A clear link thus can be built
497 between the ventilation of deep water and the sedimentary oxygenation in the OT. In
498 brief Overall, a combination of our proxy records of RSEs in core CSH1 with other

域代码已更改

带格式的: 字体: 非倾斜

域代码已更改

带格式的: 字体: 非倾斜

域代码已更改

域代码已更改

499 records shows oxygen-rich conditions during the last glaciation and middle and late
500 Holocene (since 8.5 ka) intervals, but oxygen-poor conditions during the ~~late-last~~
501 ~~deglaciation deglacial period.~~

502 6.2. Causes for sedimentary oxygenation variations

503 As discussed above, the pattern of RSEs in core CSH1 suggests that drastic
504 changes in sedimentary oxygenation occurred on orbital and millennial timescales
505 over the last glaciation in the ~~Okinawa Trough~~ OT. In general, four factors can
506 regulate the redox condition in the deep water column: (i) O₂ solubility, (ii) export
507 productivity and subsequent degradation of organic matter, (iii) vertical mixing, and
508 (iv) lateral ~~provision supply~~ of oxygen through intermediate and deeper water masses
509 (Ivanochko and Pedersen, 2004; Jaccard and Galbraith, 2012). ~~These processes have~~
510 ~~been invoked in previous studies to explain the deglacial Pacific-wide variations in~~
511 ~~oxygenation by either one or a combination of these factors~~ (Galbraith and Jaccard,
512 2015; Moffitt et al., 2015; Praetorius et al., 2015). ~~In the OT, the oxygen deficiency~~
513 ~~during the late deglacial period can be caused either by one and/or a combination of~~
514 ~~more than one of these factors.~~ Our data also suggest drastic variations in sedimentary
515 oxygenation over the last 50 ka. However, ~~In order to uncover~~ the mechanisms
516 responsible for sedimentary oxygenation variations ~~in the basin-wide OT~~ in the
517 basin-wide OT and its connection with ventilation of the open North Pacific remain
518 unclear. ~~In order to place our core results in a wider regional context, here, we~~
519 compare our proxy records of sedimentary oxygenation (U_{excess} concentration and
520 Mo/Mn ratio) and export productivity (CaCO₃) (Figures 6a, b, c) with abundance of
521 ~~Pulleniatina obliquiloculata~~ (an indicator of Kuroshio strength) and sea surface
522 temperature (Shi et al., 2014), bulk sedimentary nitrogen isotope (an indicator of
523 denitrification) (Kao et al., 2008), benthic foraminifera δ¹³C (a proxy for water mass)
524 in cores PN-3 and PC23A (Rella et al., 2012; Wahyudi and Minagawa, 1997), a proxy
525 for water mass, in core PC23A (Rella et al., 2012), abundance of benthic foraminifera
526 (an indicator of hypoxia) in core E017 (Li et al., 2005) and ODP167 site 1017
527 (Cannariato and Kennett, 1999) the NE Pacific, an indicator of anoxic condition

带格式的: 字体: (中文) 宋体

域代码已更改

带格式的: 字体: (中文) 宋体

带格式的: 字体: 小四

带格式的: 字体: (中文) 宋体

带格式的: 字体: (中文) 宋体

带格式的: 字体: (中文) 宋体

域代码已更改

域代码已更改

带格式的: 字体: (中文) 宋体

域代码已更改

带格式的: 字体: (中文) 宋体

带格式的: 字体: (中文) 宋体

带格式的: 字体: (中文) 宋体, 字体颜色: 自动设置

带格式的: 字体: (中文) 宋体

域代码已更改

带格式的: 字体: (中文) 宋体

带格式的: 字体: (中文) 宋体
带格式的: 字体: (中文) 宋体

528 ~~(Cannariato and Kennett, 1999), abundance of *Pulleniatina obliquiloculata*, an~~
529 ~~indicator of the Kuroshio strength (Shi et al., 2014)~~(Figures 6d-k).

530 6.2.1. Effects of regional ocean temperature on deglacial deoxygenation

531 Warming ocean temperatures lead to lower oxygen solubility. In the geological
532 past, solubility effects connected to temperature changes of the water column thought
533 to enhance or even trigger hypoxia (Praetorius et al., 2015). ~~For instance,~~ Shi et al.
534 (2014) reported an increase in SST of around 4°C (~21°C to ~24.6°C) during the last
535 deglaciation in core CSH1 (Figure 6d). Based on thermal solubility effects, a
536 hypothetical warming of ~~4~~1°C ~~at our site~~ would reduce oxygen concentrations by
537 about ~~8-3.5 μM/mol/kg at water temperatures around 22°C~~ (Brewer and Peltzer, 2016)
538 ~~(Benson and Krause, 1984), which therefore a ~4°C warming at core CSH1~~ (Shi et al.,
539 2014) could drive a ~~conservative estimate of a drop of <15 μmol/kg drastic in drop of~~
540 ~~oxygen concentration by assuming no large salinity changes <30 μM in subsurface~~
541 ~~water of the OT. Therefore, we assume that the late deglacial hypoxia in the OT~~
542 ~~underwent a similar increase in ocean temperatures.~~ However, given the
543 semi-quantitative nature of our data about oxygenation changes, which seemingly
544 exceed an amplitude of ~~>30-15 μmol/kgM~~, we suggest that other factors, ~~in particular~~
545 ~~processes like e.g.~~ local changes in export productivity, regional influences such as
546 vertical mixing due to changes of the Kuroshio Current, ~~as well as and~~ far-field effects
547 ~~all~~ may have played ~~some~~ decisive roles in shaping the oxygenation history of the OT.

域代码已更改
域代码已更改

域代码已更改

域代码已更改
域代码已更改
域代码已更改

548 6.2.2. Links between deglacial primary productivity and sedimentary 549 deoxygenation

550 Previous studies have suggested the occurrence of high primary productivity in
551 the entire OT during the last deglacial period (Chang et al., 2009; Jian et al., 1996;
552 Kao et al., 2008; Li et al., 2017; Shao et al., 2016; Wahyudi and Minagawa, 1997).
553 Such an increase in export production was due to favorable conditions for bloom
554 development, which were likely induced by warm temperatures and maxima in
555 nutrient availability, the latter being mainly sourced from increased discharge of the
556 Changjiang River, erosion of material from the ongoing flooding of the shallow
557 continental shelf in the ECS, and upwelling of Kuroshio Intermediate Water (Chang

域代码已更改

域代码已更改

558 et al., 2009; Li et al., 2017; Shao et al., 2016; Wahyudi and Minagawa, 1997). On the
559 basis of sedimentary reactive phosphorus concentration, Li et al. (2017) concluded
560 that export productivity increased during warm episodes but decreased during cold
561 spells on millennial timescales over the last 91 ka in the OT. Gradually increasing
562 concentrations of CaCO₃ in core CSH1 during the deglaciation (Figure 6a) and little
563 changes in foraminiferal fragmentation ratios (Wu et al., 2004), are indicative of high
564 export productivity in the northern OT. Accordingly, our data indicate that an increase
565 in export productivity during the last deglaciation, which was previously ~~reported~~
566 ~~evidenced by concentrations of reactive phosphorus~~ (Li et al., 2017) ~~and CaCO₃~~
567 ~~(Chang et al., 2009)~~ from the middle ~~and southern~~ OT ~~during the last deglaciation~~,
568 and thus was a pervasive, synchronous phenomenon of entire study region at the
569 outermost extension of the ECS.

570 ~~As a consequence, high export productivity lowers oxygen concentrations in~~
571 ~~deeper waters, due to subsurface consumption of oxygen by remineralization of~~
572 ~~organic matter.~~ Similar events of high export productivity have been ~~extensively~~
573 reported in the entire North Pacific due to increased nutrient supply, high SST,
574 reduced sea ice cover, etc. (Crusius et al., 2004; Dean et al., 1997; Galbraith et al.,
575 2007; Jaccard and Galbraith, 2012; Kohfeld and Chase, 2011). In most of these cases,
576 ~~the increase~~ds in productivity were ~~thought to be likely also~~ responsible for oxygen
577 depletion in mid-depth waters, due to exceptionally high oxygen consumption.
578 However, the productivity changes during the deglacial interval, very specifically
579 CaCO₃, are not fully consistent with the trends of excess U and Mo/Mn ratio (Figures
580 46b and 6c). The sedimentary oxygenation thus cannot be determined by export
581 productivity alone.

582 6.2.3 Effects of the Kuroshio dynamics on sedimentary oxygenation

583 The Kuroshio Current, one of the main drivers of vertical mixing, has been
584 identified as the key factor in controlling modern deep ventilation in the ~~Okinawa~~
585 ~~Trough~~OT (Kao et al., 2006). However, the ~~flow path of the Kuroshio in the Okinawa~~
586 ~~Trough~~OT during the glacial interval remains a matter of debate. Planktic
587 foraminiferal assemblages in sediment cores from inside and outside the ~~Okinawa~~

域代码已更改

域代码已更改

带格式的: 下标

域代码已更改

域代码已更改

域代码已更改

域代码已更改

588 ~~TroughOT~~ indicated that the Kuroshio have migrated to the east of the Ryukyu
589 Islands during the LGM (Ujiié and Ujiié, 1999). Subsequently, Kao et al. (2006)
590 based on modeling results suggested that the Kuroshio still enters into the ~~Okinawa~~
591 ~~TroughOT~~, but the volume transport was reduced by 43% compared to the
592 present-day transport and the outlet of Kuroshio switches from the Tokara Strait to the
593 Kerama Gap at -80 and -135m lowered sea level. Combined with sea surface
594 temperature (SST) records and ocean model results, Lee et al. (2013) argued that there
595 was little effect of deglacial sea-level change on the path of the Kuroshio, which still
596 exited the ~~Okinawa TroughOT~~ from the Tokara Strait during the glacial period.
597 Because the main stream of the Kuroshio Current is at a water depth of ~150 m, the
598 SST records are insufficient to decipher past changes of the Kuroshio (Ujiié et al.,
599 2016). On the other hand, low abundances of *P. obliquiloculata* in core CSH1 in the
600 northern OT (Figure 6e) indicate that the main flow path of the Kuroshio may have
601 migrated to the east of the Ryukyu Island (Shi et al., 2014). Such a flow change would
602 have been caused by the proposed block of the Ryukyu-Taiwan land bridge by low
603 sea level (Ujiié and Ujiié, 1999) and an overall reduced Kuroshio intensity (Kao et al.,
604 2006), effectively suppressing the effect of the Kuroshio on deep ventilation in the OT.
605 Our RSEs data show that oxygenated sedimentary conditions were dominant in the
606 northern OT throughout the last glacial period (Figures 6a, b, c, d). The Kuroshio thus
607 likely had a weak or even no effect on the renewal of oxygen to the sedimentary
608 environment during the last glacial period. More recently, lower hydrothermal total
609 Hg concentration during 20 ka - 9.6 ka, associated with reduced intensity and/or
610 variation in flow path of KC, relative to that of Holocene recorded in core KX12 - 3
611 (1423 water depth) (Lim et al., 2017), further validates our inference (Lim et al.,
612 2017).
613 On the other hand, the gradually ~~increasing~~increased alkenone-derived SST and
614 abundance of *P.obliquiloculata* (Figures 6d and 6e) from 15 ka onwards indicates an
615 intensified Kuroshio Current. ~~At present, mooring and float observations revealed~~
616 that the KC penetrates to 1200 m isobath in the East China Sea (Andres et al., 2015).
617 ~~Matsumoto et al. (2002) suggested that the influence of the present Kuroshio can~~

域代码已更改

618 ~~reach to the bottom depth of the permanent thermocline, which is approximately at~~
619 ~~1000 m water depth.~~ However, as mentioned above, the effect of Kuroshio on the
620 sedimentary oxygenation was likely very limited during the glacial period and only
621 gradually increasing throughout the last glacial termination. Therefore, while its effect
622 on our observed deglacial variation in oxygenation may provide a slowly changing
623 background condition in vertical mixing effects on the sedimentary oxygenation in the
624 OT, it cannot account for the first order, rapid oxygenation changes, including
625 indications for millennial-scale variations, that we observe between 18 ka and 9 ka,
626 ~~including indications for millennial-scale variations (Figure 6).~~

627 Better oxygenated sedimentary conditions since 8.5 ka coincided with intensified
628 Kuroshio (Li et al., 2005; Shi et al., 2014), as indicated by rapidly increased SST and
629 *P. obliquiloculata* abundance in core CSH1 (Figures 6d and 6e) and *C. hyaline*
630 abundance in core E017 (Figure 6i). ~~The r~~Re-entrance of the Kuroshio into the OT
631 (Shi et al., 2014) with rising eustatic sea level likely enhanced the vertical mixing and
632 exchange between bottom and surface waters, ventilating the deep water in the OT.
633 Previous comparative studies based on epibenthic $\delta^{13}\text{C}$ values indicated
634 well-ventilated deep water feeding both inside the OT and outside off the Ryukyu
635 Islands during the Holocene (Kubota et al., 2015; Wahyudi and Minagawa, 1997). In
636 summary, ~~during the Holocene our observed~~ enhanced sedimentary oxygenation
637 regime observed in the OT during the Holocene is mainly related to the intensified
638 Kuroshio, while the effect of the Kuroshio on OT oxygenation was limited before 15
639 ka.

640 **6.2.4. Effects of GNPIW on sedimentary oxygenation**

641 Relatively stronger oxygenated Glacial North Pacific Intermediate Water
642 (GNPIW), coined by (Matsumoto et al., 2002), has been widely documented in the
643 Bering Sea (Itaki et al., 2012; Kim et al., 2011; Rella et al., 2012), the Okhotsk Sea
644 (Itaki et al., 2008; Okazaki et al., 2014; Okazaki et al., 2006; Wu et al., 2014), off east
645 Japan (Shibahara et al., 2007), the eastern North Pacific (Cartapanis et al., 2011;
646 Ohkushi et al., 2013) and western subarctic Pacific (Keigwin, 1998; Matsumoto et al.,
647 2002). The intensified ~~ventilation-formation~~ of GNPIW due to the displacement of

域代码已更改

带格式的: 字体: 倾斜

域代码已更改

域代码已更改

域代码已更改

域代码已更改

域代码已更改

域代码已更改

域代码已更改

域代码已更改

648 ~~source region to the Bering Sea is firstly attributable to~~ was proposed by the
649 ~~displacement of formation source region to the Bering Sea~~ Ohkushi et al. (2003) and
650 ~~then and then is further~~ confirmed by Horikawa et al. (2010). Under such conditions,
651 the invasion of well-ventilated GNPIW into the OT through the Kerama Gap would
652 have replenished the water column oxygen in the OT, although the penetration depth
653 of GNPIW remains under debate (Jaccard and Galbraith, 2013; Okazaki et al., 2010;
654 Rae et al., 2014). Both a gradual decrease in excess U concentration and an increase
655 in Mo/Mn ratio during the last glacial period (25 ka-50 ka) validate such inference,
656 suggesting pronounced effects of intensified GNPIW formation in the OT.

657 During HS1, a stronger formation of GNPIW was supported by proxy studies
658 and numerical simulations(Chikamoto et al., 2012; Gong et al., 2019; Jaccard and
659 Galbraith, 2013; Max et al., 2014; Okazaki et al., 2010), recorded in the North Pacific
660 by a variety of studies.~~For example,~~ On the basis of paired benthic-planktic (B-P)
661 ¹⁴C data, ~~and model simulations, nhanced penetration of~~ Okazaki et al. (2010)
662 suggested that NPIW penetrated into a much deeper water depth ~~of ~2500 to 3000 m~~
663 during HS1 relative to the Holocene has been revealed in several studies (Max et al.,
664 2014; Okazaki et al., 2010; Sagawa and Ikehara, 2008), which was also simulated by
665 several models (Chikamoto et al., 2012; Gong et al., 2019; Okazaki et al., 2010). On
666 the other hand, increased intermediate water temperature in the subtropical Pacific
667 recorded in core GH08-2004 (1166 m water depth) (Kubota et al., 2015) and young
668 deep water observed in the northern South China Sea during HS1 (Wan and Jian,
669 2014) along downstream region of NPIW are also related to intensified NPIW
670 formation. Furthermore, In contrast, Max et al. (2014) argued against deep water
671 formation in the North Pacific and showed that GNPIW was well ventilated only to
672 intermediate water depths (< 1400 m). Various mid and high latitude North Pacific
673 records of B-P ¹⁴C age offsets at the intermediate water depth (<600-2000 m) showed
674 an active production of GNPIW during HS1 (Max et al., 2014; Sagawa and Ikehara,
675 2008). (Kubota et al., 2015)Moreover, Kubota et al. (2010) reported increased
676 subsurface water temperatures related to enhanced GNPIW contributions during HS1
677 at a water depth of 1166m (GH08, and young deep water was observed in the northern

域代码已更改

678
679
680
681
682
683
684
685
686
687
688
689
690
691
692
693
694
695
696
697
698
699
700
701
702
703
704
705
706
707

~~South China Sea during HS1 (Wan and Jian, 2014).~~
All these multiple lines of evidence imply the presence of well ventilated intermediate water in the upper 2000 m of the North Pacific during HS1. At this point, the effect of a strong GNPIW likely reached the South China Sea (Wan and Jian, 2014; Zheng et al., 2016), further to the south the Okinawa Trough. The pathway of GNPIW from numerical model simulations (Zheng et al., 2016) was similar to modern observations (You, 2003). Thus, all these evidence imply a persistent, cause and effect relation ~~has been established~~ between GNPIW ventilation, the intermediate and deep water oxygen concentration in the of OT deepwater and sediment redox state during HS1. In addition, our RSEs data also suggested a similarly enhanced ventilation in HS2 (Figures 6b and 6c) (Figure 6) that ~~must is also also be~~ attributed to intensified GNPIW.

Hypoxic conditions during ~~the Bølling-Allerød (B/A)~~ have been also widely observed in the mid- and high-latitude North Pacific (Jaccard and Galbraith, 2012; Praetorius et al., 2015). Our data, ~~both of~~ excess U concentrations and Mo/Mn ratio recorded in core CSH1 (Figures 6b- and 6c), together with enhanced denitrification and *B. aculeata* abundance (Figures 6f and 6h), further reveal the expansion of oxygen-depletion at mid-depth waters down to the subtropical NW Pacific during the late deglacial period. Based on high relative abundances of radiolarian species, indicators of upper intermediate water ventilation in core PC-23A, Itaki et al. (2012) suggested that a presence of well-ventilated waters was limited to the upper intermediate layer (200 m–500 m) in the Bering Sea during warm periods, such as the B/A and Preboreal. Higher B-P foraminiferal ¹⁴C ages, together with increased temperature and salinity at intermediate waters ~~temperature and salinity~~ recorded in core GH02-1030 (off East Japan) supported a weakened formation of NPIW during the B/A (Sagawa and Ikehara, 2008). These lines of evidence indicate that the boundary between GNPIW and North Pacific Deep Water shoaled during the B/A, in comparison to HS1. Based on a comparison of two benthic foraminiferal oxygen and carbon isotope records from off northern Japan and the southern Ryukyu Island, Kubota et al. (2015) found a stronger influence of Pacific Deep Water on

域代码已更改
域代码已更改

域代码已更改
域代码已更改
域代码已更改

域代码已更改
域代码已更改

域代码已更改

带格式的：字体：倾斜

域代码已更改

域代码已更改

域代码已更改
域代码已更改

708 intermediate-water temperature and ventilation at their southern than the northern
709 locations, although both sites are located at similar water depths (1166 m and -1212
710 m for cores GH08-2004 and GH02-1030, 1212 m, respectively). Higher excess U
711 concentration and low Mo/Mn ratio in our core CSH1 during the B/A and Preboreal
712 suggest reduced sedimentary oxygenation, consistent with reduced ventilation of
713 GNPIW, contributing to the subsurface water suboxia-deoxygenation in the OT.

714 During the YD, both Mo/Mn ratio and excess U show a slightly decreased
715 oxygen condition in the northern OT. ~~In-By~~ contrast, benthic foraminiferal $\delta^{18}\text{O}$ and
716 $\delta^{13}\text{C}$ values in a sediment core collected from the Oyashio region suggested a
717 strengthened formation and ventilation of GNPIW during the YD (Ohkushi et al.,
718 2016). This pattern possibly indicates a time-dependent, varying contribution of distal
719 GNPIW to the deglacial OT oxygenation history, and we presume a more pronounced
720 contribution of organic matter degradation due to high export productivity during this
721 period, as suggested by increasing CaCO_3 content.

722 6.3. Subtropical North Pacific ventilation links to North Atlantic Climate

723 One of the characteristics climate features in the Northern Hemisphere, in
724 particular the North Atlantic is millennial-scale oscillations during the glacial and
725 deglacial periods. These abrupt climatic events have been widely thought to be related
726 to varying strength of Atlantic Meridional Overturning Circulation (AMOC)
727 (Lynch-Stieglitz, 2017). One of dynamic proxies of ocean circulation, $^{231}\text{Pa}/^{230}\text{Th}$
728 reveals that severe weakening of AMOC only existed during Heinrich stadials due to
729 increased freshwater discharges into the North Atlantic (Böhm et al., 2015; McManus
730 et al., 2004). On the other hand, several mechanisms, such as sudden termination of
731 freshwater input (Liu et al., 2009), atmospheric CO_2 concentration (Zhang et al.,
732 2017), enhanced advection of salt (Barker et al., 2010) (Liu et al., 2009) and changes
733 in background climate (Knorr and Lohmann, 2007) were proposed to explain the
734 reinvigoration of AMOC during the B/A.

735 Our RSEs data in the Northern OT and epibenthic $\delta^{13}\text{C}$ in the Bering Sea
736 (Figures 7a-c) both show a substantial millennial variability in intermediate water
737 ventilation in the subtropical North Pacific. Notably, both enhanced ventilation during

域代码已更改

带格式的: 字体: 小四

带格式的: 缩进: 首行缩进: 2 字符

带格式的: 字体: 小四

域代码已更改

带格式的: 字体: 小四

域代码已更改

域代码已更改

带格式的: 下标

域代码已更改

域代码已更改

域代码已更改

域代码已更改

域代码已更改

带格式的: 字体: (默认) Times New Roman, (中文) +中文正文

带格式的: 上标

738 HS1 and HS2 and oxygen-poor condition during the B/A respectively correspond to
739 the collapse and resumption of ~~Atlantic meridional overturning circulation (AMOC)~~
740 ~~(Bohm et al., 2015; McManus et al., 2004)~~ (Figure 7-d). ~~Such out-of-phase~~
741 ~~millennial-scale pattern~~ This is consistent with the results of various modeling
742 simulations (Chikamoto et al., 2012; Menviel et al., 2014; Okazaki et al., 2010;
743 Saenko et al., 2004), although these models had different ~~scenarios-boundary~~
744 ~~conditions~~ and causes for the observed effects in GNPIW formation, and ventilation
745 ages derived from B-P ¹⁴C (Freeman et al., 2015; Max et al., 2014; Okazaki et al.,
746 2012). These lines of evidence ~~reveal-confirm~~ a persistent link between the ventilation
747 of North Pacific and the North Atlantic climate (Lohmann et al., 2019). Such links
748 have also been corroborated by ~~using~~ proxy data and modeling experiment between
749 AMOC and East Asian monsoon during the 8.2 ka event (Liu et al., 2013), the
750 Holocene (Wang et al., 2005) and 34 ~~ka~~-60 ka (Sun et al., 2012). The mechanism
751 linking East Asia with North Atlantic has been attributed to an atmospheric
752 teleconnection, such as the position and strength of Westerly Jet and
753 Mongolia-Siberian High (Porter and Zhisheng, 1995). However, the mechanism
754 behind such ~~oceanic ventilation seesaw out-of-phase~~ pattern between the ~~ventilation~~
755 ~~in the subtropical North Pacific and the~~ North Atlantic ~~deep water formation and~~
756 ~~North Pacific is still remains~~ unclear.

757 Increased NPIW formation ~~of-during~~ HS1 may have been caused by enhanced
758 salinity-driven vertical mixing through higher meridional water mass transport from
759 the subtropical Pacific. Previous studies have proposed that intermediate water
760 formation in the North Pacific hinged on a basin-wide increase in sea surface salinity
761 driven by changes in strength of the summer EAM and the moisture transport from
762 the Atlantic to the Pacific (Emile-Geay et al., 2003). Several modeling studies found
763 that freshwater forcing in the North Atlantic could cause a widespread surface
764 salinification in the subtropical Pacific Ocean (Menviel et al., 2014; Okazaki et al.,
765 2010; Saenko et al., 2004). This idea has been tested by proxy data (Rodríguez-Sanz
766 et al., 2013; Sagawa and Ikehara, 2008), which indicated a weakened summer EAM
767 and reduced transport of moisture from Atlantic to Pacific through Panama Isthmus

域代码已更改

768 | owing to the southward displacement of Intertropical Convergence Zone ~~ICZ~~ caused
769 | by a weakening of AMOC. Along with this process, as predicted through a general
770 | circulation modeling, a strengthened Pacific Meridional Overturning Circulation
771 | would have transported more warm and salty subtropical water into the high-latitude
772 | North Pacific (Okazaki et al., 2010). In accordance with comprehensive Mg/Ca
773 | ratio-based salinity reconstructions, however, Riethdorf et al. (2013) found no clear
774 | evidence for such higher salinity patterns in the subarctic northwest Pacific during
775 | HS1.

776 | On the other hand, a weakened AMOC would deepen the wintertime Aleutian
777 | Low based on modern observation (Okumura et al., 2009), which is closely related to
778 | the sea ice formation in the marginal seas of the subarctic Pacific (Cavalieri and
779 | Parkinson, 1987). Once stronger Aleutian Low, Intense-intense brine rejection due to-
780 | accompanied by expanded sea ice expansionformation, would have enhanced the
781 | NPIW formation. Recently our modeling-derived evidence suggests-confirms that
782 | enhanced sea ice coverage occurred in the southern Okhotsk Sea and off East
783 | Kamchatka Peninsula during HS1 (Gong et al., 2019). In addition, higher-stronger
784 | advection of low-salinity water via the Alaskan Stream to the subarctic NW Pacific
785 | was probably enhanced during HS1, related to a shift of the Aleutian Low pressure
786 | system over the North Pacific, which could also increase sea ice formation, brine
787 | rejection and thereafter intermediate water ventilation (Riethdorf et al., 2013).

788 | During the late deglaciation, ameliorating global climate conditions, such as
789 | warming Northern Hemisphere, and a strengthened Asian summer monsoon, are a
790 | result of changes in insolation forcing, greenhouse gases concentrations, and variable
791 | strengths of the AMOC (Clark et al., 2012; Liu et al., 2009). During the B/A, a
792 | decrease in sea ice extent and duration, as well as reduced advection of Alaska Stream
793 | waters were indicated by combined reconstructions of SST and mixed layer
794 | temperatures from the subarctic Pacific (Riethdorf et al., 2013). At that time, the
795 | rising eustatic sea level (Spratt and Lisiecki, 2016) would have supported the
796 | intrusion of Alaska Stream into the Bering Sea by deepening and opening glacial
797 | closed straits of the Aleutian Islands chain, while reducing the advection of the Alaska

域代码已更改

域代码已更改

域代码已更改

域代码已更改

域代码已更改

域代码已更改

域代码已更改

域代码已更改

域代码已更改

798 Stream to the subarctic Pacific gyre (Riethdorf et al., 2013). In this scenario, saltier
799 and more stratified surface water conditions would have inhibited brine rejection and
800 subsequent formation and ventilation of NPIW (Lam et al., 2013), leading to a
801 reorganization of the Pacific water mass, closely coupled to the collapse and
802 resumption modes of the AMOC during these two intervals.

803 **6.4 Increased storage of CO₂ at mid-depth water in the North Pacific at the B/A**

804 One of the striking features of RSEs data is higher Mo/Mn ratios and excess U
805 concentrations at the B/A, ~~indicating supporting an expansion of Oxygen Minimum~~
806 ~~Zone a substantial oxygen poor condition in the subtropical~~ North Pacific (Galbraith
807 ~~and Jaccard, 2015; Jaccard and Galbraith, 2012; Moffitt et al., 2015) and~~ coinciding
808 with the termination of atmospheric CO₂ concentration rise (Marcott et al., 2014)
809 (Figure 7a7e). As described above, it can be related to the upwelling of nutrient- and
810 CO₂-rich Pacific Deep Water due to resumption of AMOC and enhanced export
811 production. Although here we are unable to distinguish these two reasons from each
812 other, boron isotope data measured on surface-dwelling foraminifera in core
813 MD01-2416 situated in the western subarctic North Pacific did reveal a decrease in
814 near-surface pH and an increase in pCO₂ at this time (Gray et al., 2018). That is to say,
815 subarctic North Pacific is a source of relatively high atmospheric CO₂ concentration at
816 the B/A. Here we cannot conclude that the same processes could have occurred in the
817 subtropical North Pacific due to the lack of well-known drivers to draw out of the old
818 carbon in the deep sea into the atmosphere. However, an expansion of
819 oxygen-depletion zone in the entire North Pacific suggest an increase in respired
820 carbon storage at intermediate-depth in the subtropical North Pacific, which likely
821 stalls the rise of atmospheric CO₂. Our results support the findings by Galbraith et al.
822 (2007) and are consistent with the hypothesis of deglacial flushing of respired carbon
823 dioxide from an isolated, deep ocean reservoir (Marchitto et al., 2007; Sigman and
824 Boyle, 2000). Given the sizeable volume of the North Pacific, potentially, once the
825 respired carbon could be emitted to the atmosphere in stages, which would play an
826 important role in propelling the Earth out of the last ice age (Jaccard and Galbraith,
827 2018).

域代码已更改

域代码已更改

域代码已更改

域代码已更改

域代码已更改

域代码已更改

域代码已更改

828 **7. Conclusions**

829 Our geochemical results of sediment core CSH1 revealed substantial changes in
830 intermediate water redox conditions in the northern Okinawa Trough over the last 50
831 ka on orbital and millennial timescales ~~in the past~~. Enhanced sedimentary oxygenation
832 mainly occurred during cold intervals, such as the last glacial period, Heinrich stadials
833 1 and 2, and during the middle and late Holocene, while diminished sedimentary
834 oxygenation prevailed during the Bölling-Alleröd and Preboreal. The sedimentary
835 oxygenation variability presented here provides key evidence for the substantial
836 impact of ventilation of NPIW on the sedimentary oxygenation in the subtropical
837 North Pacific and ~~highlights~~ shows out-of-phase pattern with North Atlantic Climate
838 during the last deglaciation ~~the major role of Atlantic Meridional Overturning~~
839 ~~Circulation in regulating the variations in sedimentary oxygenation in the Okinawa~~
840 ~~Trough through ventilation of NPIW~~. The linkage is attributable to the disruption of
841 NPIW formation caused by climate changes in the North Atlantic, which is transferred
842 to the North Pacific via atmospheric and oceanic teleconnections. ~~Combined with~~
843 ~~other published records~~, We also suggest an expansion of oxygen-depleted zone and
844 accumulation of respired carbon at the mid-depth waters of the North Pacific at during
845 the B/A, coinciding with the termination of atmospheric CO₂ rise. A step-wise
846 injection of such respired carbon into the atmosphere, mechanism likely to propel the
847 Earth out of glacial climate, would be helpful to maintain high atmospheric CO₂
848 levels during the deglaciation.

带格式的: 字体: 小四

带格式的: 字体: 小四, 下标

带格式的: 字体: 小四

849 ~~Once the release of the sequestered carbon into the atmosphere in stages, it would~~
850 ~~be helpful to maintain high atmospheric CO₂ levels during the deglaciation and to~~
851 ~~propel the earth out of the glacial climate.~~

852

853 **Data availability.** All raw data are available to all interested researchers upon request.

854

855 **Author Contributions.** J.J.Z. and X.F.S. conceived the study. A.M.Z. performed
856 geochemical analyses of bulk sediments. J.J.Z., X.F.S. K.S. and X.G. led the write up
857 of the manuscript. All other authors provided comments on the manuscript and

858 contributed to the final version of the manuscript.

859

860 **Competing interests:** The authors declare no competing interests.

861

862 **Acknowledgements**

863 Financial support was provided by the National Program on Global Change and
864 Air-Sea Interaction (GASI-GEOGE-04), by the National Natural Science Foundation
865 of China (Grant Nos.: 41476056, 41876065, 41420104005, 41206059, and U1606401)
866 and by the Basic Scientific Fund for National Public Research Institutes of China
867 (No.2016Q09) and International Cooperative Projects in Polar Study (201613) and
868 Taishan Scholars Program of Shandong. This study is a contribution to the bilateral
869 Sino-German collaboration project (funding through BMBF grant 03F0704A –
870 SIGEPAX). XG, LLJ, GL, RT thank the bilateral Sino-German collaboration
871 NOPAWAC project (BMBF grant No. 03F0785A).LLJ and RT acknowledge financial
872 support through the national Helmholtz REKLIM Initiative. We would like to thank
873 the anonymous reviewers, who helped to improve the quality of this manuscript. The
874 data used in this study are available from the authors upon request
875 (zoujianjun@fio.org.cn).

876

877 **References**

- 878 Addison, J. A., Finney, B. P., Dean, W. E., Davies, M. H., Mix, A. C., Stoner, J. S., and Jaeger, J. M.:
879 Productivity and sedimentary $\delta^{15}\text{N}$ variability for the last 17,000 years along the northern Gulf of
880 Alaska continental slope, *Paleoceanography*, 27, PA1206, doi:10.1029/2011PA002161, 2012.
- 881 Algeo, T. J.: Can marine anoxic events draw down the trace element inventory of seawater?, *Geology*,
882 32, 1057-1060, 2004.
- 883 Algeo, T. J. and Lyons, T. W.: Mo-total organic carbon covariation in modern anoxic marine
884 environments: Implications for analysis of paleoredox and paleohydrographic conditions,
885 *Paleoceanography*, 21, PA1016, doi: 10.1029/2004pa001112, 2006.
- 886 Algeo, T. J. and Tribouillard, N.: Environmental analysis of paleoceanographic systems based on
887 molybdenum - uranium covariation, *Chemical Geology*, 268, 211-225, 2009.
- 888 Andres, M., Jan, S., Sanford, T. B., Mensah, V., Centurioni, L. R., and Book, J. W.: Mean structure and
889 variability of the Kuroshio from northeastern Taiwan to southwestern Japan, *Oceanography*, 26, 84-95,
890 2015.
- 891 Böhm, E., Lippold, J., Gutjahr, M., Frank, M., Blaser, P., Antz, B., Fohlmeister, J., Frank, N., Andersen,

域代码已更改

892 M. B., and Deining, M.: Strong and deep Atlantic meridional overturning circulation during the last
893 glacial cycle, *Nature*, 517, 73-76, 2015.

894 Barker, S., Knorr, G., Vautravers, M. J., Diz, P., and Skinner, L. C.: Extreme deepening of the Atlantic
895 overturning circulation during deglaciation, *Nature Geoscience*, 3, 567-571, 2010.

896 Bianchi, D., Dunne, J. P., Sarmiento, J. L., and Galbraith, E. D.: Data-based estimates of suboxia,
897 denitrification, and N₂O production in the ocean and their sensitivities to dissolved O₂, *Global*
898 *Biogeochemical Cycles*, 26, doi:10.1029/2011gb004209, 2012.

899 Brewer, P. G. and Peltzer, E. T.: Ocean chemistry, ocean warming, and emerging hypoxia: Commentary,
900 *Journal of Geophysical Research: Oceans*, 121, 3659-3667, 2016.

901 Burdige, D. J.: The biogeochemistry of manganese and iron reduction in marine sediments,
902 *Earth-Science Reviews*, 35, 249-284, 1993.

903 Cannariato, K. G. and Kennett, J. P.: Climatically related millennial-scale fluctuations in strength of
904 California margin oxygen-minimum zone during the past 60 k.y, *Geology*, 27, 975-978, 1999.

905 Cartapanis, O., Tachikawa, K., and Bard, E.: Northeastern Pacific oxygen minimum zone variability
906 over the past 70 kyr: Impact of biological production and oceanic ventilation, *Paleoceanography*, 26,
907 PA4208, doi: 4210.1029/2011PA002126, 2011.

908 Cavalieri, D. J. and Parkinson, C. L.: On the relationship between atmospheric circulation and the
909 fluctuations in the sea ice extents of the bering and okhotsk seas, *Journal of Geophysical*
910 *Research-Oceans*, 92, 7141-7162, 1987.

911 Chang, A. S., Pedersen, T. F., and Hندی, I. L.: Effects of productivity, glaciation, and ventilation on
912 late Quaternary sedimentary redox and trace element accumulation on the Vancouver Island margin,
913 western Canada, *Paleoceanography*, 29, doi: 10.1002/2013PA002581, 2014.

914 Chang, Y.-P., Chen, M.-T., Yokoyama, Y., Matsuzaki, H., Thompson, W. G., Kao, S.-J., and Kawahata,
915 H.: Monsoon hydrography and productivity changes in the East China Sea during the past 100,000
916 years: Okinawa Trough evidence (MD012404), *Paleoceanography*, 24, PA3208, doi:
917 3210.1029/2007PA001577, 2009.

918 Chen, J., Zhang, D., Zhang, W., and Li, T.: The paleoclimatic change since the last galciation in the
919 north of Okinawa Trough based on the spore-pollen records, *Acta Oceanologica Sinica*, 28, 85-91(in
920 Chinese with English Abstract), 2006.

921 Cheng, H., Edwards, R. L., Sinha, A., Spötl, C., Yi, L., Chen, S., Kelly, M., Kathayat, G., Wang, X., Li,
922 X., Kong, X., Wang, Y., Ning, Y., and Zhang, H.: The Asian monsoon over the past 640,000 years and
923 ice age terminations, *Nature*, 534, 640-646, 2016.

924 Cheng, H., Edwards, R. L., Southon, J., Matsumoto, K., Feinberg, J. M., Sinha, A., Zhou, W., Li, H., Li,
925 X., Xu, Y., Chen, S., Tan, M., Wang, Q., Wang, Y., and Ning, Y.: Atmospheric 14C/12C changes during
926 the last glacial period from Hulu Cave, *Science*, 362, 1293-1297, 2018.

927 Chikamoto, M. O., Menviel, L., Abe-Ouchi, A., Ohgaito, R., Timmermann, A., Okazaki, Y., Harada, N.,
928 Oka, A., and Mouchet, A.: Variability in North Pacific intermediate and deep water ventilation during
929 Heinrich events in two coupled climate models, *Deep Sea Research Part II: Topical Studies in*
930 *Oceanography*, 61-64, 114-126, 2012.

931 Clark, P. U., Shakun, J. D., Baker, P. A., Bartlein, P. J., Brewer, S., Brook, E., Carlson, A. E., Cheng, H.,
932 Kaufman, D. S., Liu, Z., Marchitto, T. M., Mix, A. C., Morrill, C., Otto-Bliesner, B. L., Pahnke, K.,
933 Russell, J. M., Whitlock, C., Adkins, J. F., Blois, J. L., Clark, J., Colman, S. M., Curry, W. B., Flower,
934 B. P., He, F., Johnson, T. C., Lynch-Stieglitz, J., Markgraf, V., McManus, J., Mitrovica, J. X., Moreno, P.
935 I., and Williams, J. W.: Global climate evolution during the last deglaciation, *Proceedings of the*

936 National Academy of Sciences of the United States of America, 109, E1134-E1142, 2012.

937 Clemens, S. C., Holbourn, A., Kubota, Y., Lee, K. E., Liu, Z., Chen, G., Nelson, A., and Fox-Kemper,
938 B.: Precession-band variance missing from East Asian monsoon runoff, *Nature Communications*, 9,
939 3364, doi: 3310.1038/s41467-41018-05814-41460, 2018.

940 Crusius, J., Calvert, S., Pedersen, T., and Sage, D.: Rhenium and molybdenum enrichments in
941 sediments as indicators of oxic, suboxic and sulfidic conditions of deposition, *Earth and Planetary
942 Science Letters*, 145, 65-78, 1996.

943 Crusius, J., Pedersen, T. F., Kienast, S., Keigwin, L., and Labeyrie, L.: Influence of northwest Pacific
944 productivity on North Pacific Intermediate Water oxygen concentrations during the Boiling-Allerod
945 interval (14.7-12.9 ka), *Geology*, 32, 633-636, 2004.

946 Dahl, T. W., Anbar, A. D., Gordon, G. W., Rosing, M. T., Frei, R., and Canfield, D. E.: The behavior of
947 molybdenum and its isotopes across the chemocline and in the sediments of sulfidic Lake Cadagno,
948 Switzerland, *Geochimica et Cosmochimica Acta*, 74, 144-163, 2010.

949 Dean, W. E., Gardner, J. V., and Piper, D. Z.: Inorganic geochemical indicators of glacial-interglacial
950 changes in productivity and anoxia on the California continental margin, *Geochimica et Cosmochimica
951 Acta*, 61, 4507-4518, 1997.

952 Delcroix, T. and Murtugudde, R.: Sea surface salinity changes in the East China Sea during 1997–2001:
953 Influence of the Yangtze River, *Journal of Geophysical Research: Oceans*, 107, 8008,
954 doi:8010.1029/2001JC000893, 2002.

955 Dou, Y., Yang, S., Li, C., Shi, X., Liu, J., and Bi, L.: Deepwater redox changes in the southern Okinawa
956 Trough since the last glacial maximum, *Progress in Oceanography*, 135, 77-90, 2015.

957 Emile-Geay, J., Cane, M. A., Naik, N., Seager, R., Clement, A. C., and van Geen, A.: Warren revisited:
958 Atmospheric freshwater fluxes and “Why is no deep water formed in the North Pacific”, *Journal of
959 Geophysical Research: Oceans*, 108, doi:10.1029/2001JC001058, 2003.

960 Freeman, E., Skinner, L. C., Tisserand, A., Dokken, T., Timmermann, A., Menviel, L., and Friedrich, T.:
961 An Atlantic–Pacific ventilation seesaw across the last deglaciation, *Earth and Planetary Science Letters*,
962 424, 237-244, 2015.

963 Galbraith, E. D. and Jaccard, S. L.: Deglacial weakening of the oceanic soft tissue pump: global
964 constraints from sedimentary nitrogen isotopes and oxygenation proxies, *Quaternary Science Reviews*,
965 109, 38-48, 2015.

966 Galbraith, E. D., Jaccard, S. L., Pedersen, T. F., Sigman, D. M., Haug, G. H., Cook, M., Southon, J. R.,
967 and Francois, R.: Carbon dioxide release from the North Pacific abyss during the last deglaciation,
968 *Nature*, 449, 890-893, 2007.

969 Galbraith, E. D., Kienast, M., Pedersen, T. F., and Calvert, S. E.: Glacial-interglacial modulation of the
970 marine nitrogen cycle by high-latitude O₂ supply to the global thermocline, *Paleoceanography*, 19,
971 PA4007, doi:4010.1029/2003PA001000, 2004.

972 Ge, S., Shi, X., Wu, Y., Lee, T., Xiong, Y., and Saito, Y.: Rock magnetic property of gravity core CSH1
973 from the northern Okinawa Trough and the effect of early diagenesis, *Acta Oceanologica Sinica*, 26,
974 54-65, 2007.

975 Gong, X., Lembke-Jene, L., Lohmann, G., Knorr, G., Tiedemann, R., Zou, J. J., and Shi, X. F.:
976 Enhanced North Pacific deep-ocean stratification by stronger intermediate water formation during
977 Heinrich Stadial 1, *Nature Communications*, 10, 656, doi:610.1038/s41467-41019-08606-41462, 2019.

978 Gray, W. R., Rae, J. W. B., Wills, R. C. J., Shevenell, A. E., Taylor, B., Burke, A., Foster, G. L., and
979 Lear, C. H.: Deglacial upwelling, productivity and CO₂ outgassing in the North Pacific Ocean, *Nature*

980 Geoscience, 11, 340-344, 2018.

981 Helz, G. R., Miller, C. V., Charnock, J. M., Mosselmans, J. F. W., Patrick, R. A. D., Garner, C. D., and
982 Vaughan, D. J.: Mechanism of molybdenum removal from the sea and its concentration in black shales:
983 EXAFS evidence, *Geochimica et Cosmochimica Acta*, 60, 3631-3642, 1996.

984 Hofmann, A. F., Peltzer, E. T., Walz, P. M., and Brewer, P. G.: Hypoxia by degrees: Establishing
985 definitions for a changing ocean, *Deep Sea Research Part I: Oceanographic Research Papers*, 58,
986 1212-1226, 2011.

987 Hoogakker, B. A. A., Elderfield, H., Schmiedl, G., McCave, I. N., and Rickaby, R. E. M.:
988 Glacial–interglacial changes in bottom-water oxygen content on the Portuguese margin, *Nature*
989 *Geoscience*, 8, 40-43, 2015.

990 Horikawa, K., Asahara, Y., Yamamoto, K., and Okazaki, Y.: Intermediate water formation in the Bering
991 Sea during glacial periods: Evidence from neodymium isotope ratios, *Geology*, 38, 435-438, 2010.

992 Ichikawa, H. and Beardsley, R. C.: The Current System in the Yellow and East China Seas, *Journal of*
993 *Oceanography*, 58, 77-92, 2002.

994 Itaki, T., Khim, B. K., and Ikehara, K.: Last glacial-Holocene water structure in the southwestern
995 Okhotsk Sea inferred from radiolarian assemblages, *Marine Micropaleontology*, 67, 191-215, 2008.

996 Itaki, T., Kim, S., Rella, S. F., Uchida, M., Tada, R., and Khim, B. K.: Millennial-scale variations of
997 late Pleistocene radiolarian assemblages in the Bering Sea related to environments in shallow and deep
998 waters, *Deep-Sea Research Part II-Topical Studies in Oceanography*, 61-64, 127-144, 2012.

999 Ivanochko, T. S. and Pedersen, T. F.: Determining the influences of Late Quaternary ventilation and
1000 productivity variations on Santa Barbara Basin sedimentary oxygenation: a multi-proxy approach,
1001 *Quaternary Science Reviews*, 23, 467-480, 2004.

1002 Jaccard, S. L. and Galbraith, E. D.: Direct ventilation of the North Pacific did not reach the deep ocean
1003 during the last deglaciation, *Geophysical Research Letters*, 40, 199-203, 2013.

1004 Jaccard, S. L. and Galbraith, E. D.: Large climate-driven changes of oceanic oxygen concentrations
1005 during the last deglaciation, *Nature Geoscience*, 5, 151-156, 2012.

1006 Jaccard, S. L. and Galbraith, E. D.: Push from the Pacific, *Nature Geoscience*, 11, 299-300, 2018.

1007 Jaccard, S. L., Galbraith, E. D., Martínez-García, A., and Anderson, R. F.: Covariation of deep
1008 Southern Ocean oxygenation and atmospheric CO₂ through the last ice age, *Nature*, 530, 207-210,
1009 2016.

1010 Jaccard, S. L., Galbraith, E. D., Sigman, D. M., Haug, G. H., Francois, R., Pedersen, T. F., Dulski, P.,
1011 and Thierstein, H. R.: Subarctic Pacific evidence for a glacial deepening of the oceanic respired carbon
1012 pool, *Earth and Planetary Science Letters*, 277, 156-165, 2009.

1013 Jian, Z. M., Chen, R. H., and Li, B. H.: Deep-sea benthic foraminiferal record of the paleoceanography
1014 in the southern Okinawa trough over the last 20000 years, *Science in China Series D-Earth Sciences*,
1015 39, 551-560, 1996.

1016 Kao, S. J., Horng, C. S., Hsu, S. C., Wei, K. Y., Chen, J., and Lin, Y. S.: Enhanced deepwater
1017 circulation and shift of sedimentary organic matter oxidation pathway in the Okinawa Trough since the
1018 Holocene, *Geophysical Research Letters*, 32, L15609, doi:10.1029/2005GL023139, 2005.

1019 Kao, S. J., Liu, K. K., Hsu, S. C., Chang, Y. P., and Dai, M. H.: North Pacific-wide spreading of
1020 isotopically heavy nitrogen during the last deglaciation: Evidence from the western Pacific,
1021 *Biogeosciences*, 5, 1641-1650, 2008.

1022 Kao, S. J., Wu, C.-R., Hsin, Y.-C., and Dai, M.: Effects of sea level change on the upstream Kuroshio
1023 Current through the Okinawa Trough, *Geophysical Research Letters*, 33, L16604,

1024 doi:16610.11029/12006gl026822, 2006.

1025 Keigwin, L. D.: Glacial-age hydrography of the far northwest Pacific Ocean, *Paleoceanography*, 13,
1026 323-339, 1998.

1027 Kim, S., Khim, B. K., Uchida, M., Itaki, T., and Tada, R.: Millennial-scale paleoceanographic events
1028 and implication for the intermediate-water ventilation in the northern slope area of the Bering Sea
1029 during the last 71 kyrs, *Global and Planetary Change*, 79, 89-98, 2011.

1030 Klinkhammer, G. P. and Palmer, M. R.: Uranium in the oceans: Where it goes and why, *Geochimica et*
1031 *Cosmochimica Acta*, 55, 1799-1806, 1991.

1032 Knorr, G. and Lohmann, G.: Rapid transitions in the Atlantic thermohaline circulation triggered by
1033 global warming and meltwater during the last deglaciation, *Geochemistry, Geophysics, Geosystems*, 8,
1034 DOI: 10.1029/2007gc001604, 2007.

1035 Kohfeld, K. E. and Chase, Z.: Controls on deglacial changes in biogenic fluxes in the North Pacific
1036 Ocean, *Quaternary Science Reviews*, 30, 3350-3363, 2011.

1037 Kubota, Y., Kimoto, K., Itaki, T., Yokoyama, Y., Miyairi, Y., and Matsuzaki, H.: Bottom water
1038 variability in the subtropical northwestern Pacific from 26 kyr BP to present based on Mg/Ca and stable
1039 carbon and oxygen isotopes of benthic foraminifera, *Climate of the Past*, 11, 803-824, 2015.

1040 Kubota, Y., Kimoto, K., Tada, R., Oda, H., Yokoyama, Y., and Matsuzaki, H.: Variations of East Asian
1041 summer monsoon since the last deglaciation based on Mg/Ca and oxygen isotope of planktic
1042 foraminifera in the northern East China Sea, *Paleoceanography*, 25, PA4205,
1043 doi:4210.1029/2009pa001891, 2010.

1044 Lam, P. J., Robinson, L. F., Blusztajn, J., Li, C., Cook, M. S., McManus, J. F., and Keigwin, L. D.:
1045 Transient stratification as the cause of the North Pacific productivity spike during deglaciation, *Nature*
1046 *Geosci*, 6, 622-626, 2013.

1047 Lee, K. E., Lee, H. J., Park, J.-H., Chang, Y.-P., Ikehara, K., Itaki, T., and Kwon, H. K.: Stability of the
1048 Kuroshio path with respect to glacial sea level lowering, *Geophysical Research Letters*, 40, 392-396,
1049 doi:310.1002/grl.50102, 2013.

1050 Lembke-Jene, L., Tiedemann, R., Nürnberg, D., Kokfelt, U., Kozdon, R., Max, L., Röhl, U., and
1051 Gorbarenko, S. A.: Deglacial variability in Okhotsk Sea Intermediate Water ventilation and
1052 biogeochemistry: Implications for North Pacific nutrient supply and productivity, *Quaternary Science*
1053 *Reviews*, 160, 116-137, 2017.

1054 Li, D., Zheng, L.-W., Jaccard, S. L., Fang, T.-H., Paytan, A., Zheng, X., Chang, Y.-P., and Kao, S.-J.:
1055 Millennial-scale ocean dynamics controlled export productivity in the subtropical North Pacific,
1056 *Geology*, 45, 651-654, 2017.

1057 Li, T. G., Xiang, R., Sun, R. T., and Cao, Q. Y.: Benthic foraminifera and bottom water evolution in the
1058 middle-southern Okinawa Trough during the last 18 ka, *Science in China Series D-Earth Sciences*, 48,
1059 805-814, 2005.

1060 Li, Y. H. and Schoonmaker, J. E.: Chemical Composition and Mineralogy of Marine Sediments. In:
1061 *Treatise on Geochemistry (Second Edition)*, Turekian, K. K. (Ed.), Elsevier, Oxford, 2014.

1062 Lim, D., Kim, J., Xu, Z., Jeong, K., and Jung, H.: New evidence for Kuroshio inflow and deepwater
1063 circulation in the Okinawa Trough, East China Sea: Sedimentary mercury variations over the last
1064 20 kyr, *Paleoceanography*, 32, 571-579, 2017.

1065 Liu, Y. H., Henderson, G. M., Hu, C. Y., Mason, A. J., Charnley, N., Johnson, K. R., and Xie, S. C.:
1066 Links between the East Asian monsoon and North Atlantic climate during the 8,200 year event, *Nature*
1067 *Geosci*, 6, 117-120, 2013.

1068 Liu, Z., Otto-Bliesner, B. L., He, F., Brady, E. C., Tomas, R., Clark, P. U., Carlson, A. E.,
1069 Lynch-Stieglitz, J., Curry, W., Brook, E., Erickson, D., Jacob, R., Kutzbach, J., and Cheng, J.: Transient
1070 Simulation of Last Deglaciation with a New Mechanism for Bølling-Allerød Warming, *Science*, 325,
1071 310-314, 2009.

1072 Lohmann, G., Lembke-Jene, L., Tiedemann, R., Gong, X., Scholz, P., Zou, J., and Shi, X.: Challenges
1073 in the Paleoclimatic Evolution of the Arctic and Subarctic Pacific since the Last Glacial Period—The
1074 Sino–German Pacific–Arctic Experiment (SiGePAX), *Challenges*, 10, 13, doi:10.3390/challe10010013,
1075 2019.

1076 Lynch-Stieglitz, J.: The Atlantic Meridional Overturning Circulation and Abrupt Climate Change,
1077 *Annual Review of Marine Science*, 9, 83-104, 2017.

1078 Lyons, T. W., Anbar, A. D., Severmann, S., Scott, C., and Gill, B. C.: Tracking Euxinia in the Ancient
1079 Ocean: A Multiproxy Perspective and Proterozoic Case Study, *Annual Review of Earth and Planetary
1080 Sciences*, 37, 507-534, 2009.

1081 Machida, H.: The stratigraphy, chronology and distribution of distal marker-tephras in and around
1082 Japan, *Global and Planetary Change*, 21, 71-94, 1999.

1083 Maithani, P. B. and Srinivasan, S.: Felsic Volcanic Rocks, a Potential Source of Uranium - An Indian
1084 Overview, *Energy Procedia*, 7, 163-168, 2011.

1085 Marchitto, T. M., Lehman, S. J., Ortiz, J. D., Flückiger, J., and van Geen, A.: Marine Radiocarbon
1086 Evidence for the Mechanism of Deglacial Atmospheric CO₂ Rise, *Science*, 316, 1456-1459, 2007.

1087 Marcott, S. A., Bauska, T. K., Buizert, C., Steig, E. J., Rosen, J. L., Cuffey, K. M., Fudge, T. J.,
1088 Severinghaus, J. P., Ahn, J., Kalk, M. L., McConnell, J. R., Sowers, T., Taylor, K. C., White, J. W. C.,
1089 and Brook, E. J.: Centennial-scale changes in the global carbon cycle during the last deglaciation,
1090 *Nature*, 514, 616-619, 2014.

1091 Matsumoto, K., Oba, T., Lynch-Stieglitz, J., and Yamamoto, H.: Interior hydrography and circulation of
1092 the glacial Pacific Ocean, *Quaternary Science Reviews*, 21, 1693-1704, 2002.

1093 Max, L., Lembke-Jene, L., Riethdorf, J. R., Tiedemann, R., Nurnberg, D., Kuhn, H., and Mackensen,
1094 A.: Pulses of enhanced North Pacific Intermediate Water ventilation from the Okhotsk Sea and Bering
1095 Sea during the last deglaciation, *Climate of the Past*, 10, 591-605, 2014.

1096 McManus, J., Berelson, W. M., Klinkhammer, G. P., Hammond, D. E., and Holm, C.: Authigenic
1097 uranium: Relationship to oxygen penetration depth and organic carbon rain, *Geochimica et
1098 Cosmochimica Acta*, 69, 95-108, 2005.

1099 McManus, J. F., Francois, R., Gherardi, J. M., Keigwin, L. D., and Brown-Leger, S.: Collapse and rapid
1100 resumption of Atlantic meridional circulation linked to deglacial climate changes, *Nature*, 428, 834-837,
1101 2004.

1102 Menviel, L., England, M. H., Meissner, K. J., Mouchet, A., and Yu, J.: Atlantic-Pacific seesaw and its
1103 role in outgassing CO₂ during Heinrich events, *Paleoceanography*, 29, 58-70, 2014.

1104 Moffitt, S. E., Moffitt, R. A., Sauthoff, W., Davis, C. V., Hewett, K., and Hill, T. M.: Paleoceanographic
1105 Insights on Recent Oxygen Minimum Zone Expansion: Lessons for Modern Oceanography, *PLOS
1106 ONE*, 10, e0115246, doi, 0115210.0111371/journal.pone.0115246, 2015.

1107 Morford, J. L. and Emerson, S.: The geochemistry of redox sensitive trace metals in sediments,
1108 *Geochimica et Cosmochimica Acta*, 63, 1735-1750, 1999.

1109 Nakamura, H., Nishina, A., Liu, Z. J., Tanaka, F., Wimbush, M., and Park, J. H.: Intermediate and deep
1110 water formation in the Okinawa Trough, *Journal of Geophysical Research-Oceans*, 118, 6881-6893,
1111 2013.

1112 Nameroff, T. J., Balistrieri, L. S., and Murray, J. W.: Suboxic trace metal geochemistry in the Eastern
1113 Tropical North Pacific, *Geochimica et Cosmochimica Acta*, 66, 1139-1158, 2002.

1114 Nameroff, T. J., Calvert, S. E., and Murray, J. W.: Glacial-interglacial variability in the eastern tropical
1115 North Pacific oxygen minimum zone recorded by redox-sensitive trace metals, *Paleoceanography*, 19,
1116 PA1010, doi:10.1029/2003PA000912, 2004.

1117 Nishina, A., Nakamura, H., Park, J.-H., Hasegawa, D., Tanaka, Y., Seo, S., and Hibiya, T.: Deep
1118 ventilation in the Okinawa Trough induced by Kerama Gap overflow, *Journal of Geophysical Research:
1119 Oceans*, 121, 6092-6102, 2016.

1120 Ohkushi, K., Hara, N., Ikehara, M., Uchida, M., and Ahagon, N.: Intensification of North Pacific
1121 intermediate water ventilation during the Younger Dryas, *Geo-Mar Lett*, 36, 353-360, 2016.

1122 Ohkushi, K., Itaki, T., and Nemoto, N.: Last Glacial-Holocene change in intermediate-water ventilation
1123 in the Northwestern Pacific, *Quaternary Science Reviews*, 22, 1477-1484, 2003.

1124 Ohkushi, K., Kennett, J. P., Zeleski, C. M., Moffitt, S. E., Hill, T. M., Robert, C., Beaufort, L., and Behl,
1125 R. J.: Quantified intermediate water oxygenation history of the NE Pacific: A new benthic foraminiferal
1126 record from Santa Barbara basin, *Paleoceanography*, 28, 453-467, 2013.

1127 Okazaki, Y., Kimoto, K., Asahi, H., Sato, M., Nakamura, Y., and Harada, N.: Glacial to deglacial
1128 ventilation and productivity changes in the southern Okhotsk Sea, *Palaeogeography Palaeoclimatology
1129 Palaeoecology*, 395, 53-66, 2014.

1130 Okazaki, Y., Sagawa, T., Asahi, H., Horikawa, K., and Onodera, J.: Ventilation changes in the western
1131 North Pacific since the last glacial period, *Climate of the Past*, 8, 17-24, 2012.

1132 Okazaki, Y., Seki, O., Nakatsuka, T., Sakamoto, T., Ikehara, M., and Takahashi, K.: *Cycladophora
1133 davisiana* (Radiolaria) in the Okhotsk Sea: A key for reconstructing glacial ocean conditions, *Journal of
1134 Oceanography*, 62, 639-648, 2006.

1135 Okazaki, Y., Timmermann, A., Menviel, L., Harada, N., Abe-Ouchi, A., Chikamoto, M. O., Mouchet,
1136 A., and Asahi, H.: Deepwater Formation in the North Pacific During the Last Glacial Termination,
1137 *Science*, 329, 200-204, 2010.

1138 Okumura, Y. M., Deser, C., Hu, A., Timmermann, A., and Xie, S.-P.: North Pacific Climate Response to
1139 Freshwater Forcing in the Subarctic North Atlantic: Oceanic and Atmospheric Pathways, *Journal of
1140 Climate*, 22, 1424-1445, 2009.

1141 Porter, S. C. and Zhisheng, A.: Correlation between climate events in the North Atlantic and China
1142 during the last glaciation, *Nature*, 375, 305-308, 1995.

1143 Praetorius, S. K., Mix, A. C., Walczak, M. H., Wolhowe, M. D., Addison, J. A., and Prah, F. G.: North
1144 Pacific deglacial hypoxic events linked to abrupt ocean warming, *Nature*, 527, 362-366, 2015.

1145 Qu, T. and Lukas, R.: The Bifurcation of the North Equatorial Current in the Pacific, *Journal of
1146 Physical Oceanography*, 33, 5-18, 2003.

1147 Rühlemann, C., Müller, P. J., and Schneider, R. R.: Organic Carbon and Carbonate as Paleoproductivity
1148 Proxies: Examples from High and Low Productivity Areas of the Tropical Atlantic. In: *Use of Proxies
1149 in Paleoceanography: Examples from the South Atlantic*, Fischer, G. and Wefer, G. (Eds.), Springer
1150 Berlin Heidelberg, Berlin, Heidelberg, 1999.

1151 Rae, J. W. B., Sarnthein, M., Foster, G. L., Ridgwell, A., Grootes, P. M., and Elliott, T.: Deep water
1152 formation in the North Pacific and deglacial CO₂ rise, *Paleoceanography*, 29, 645-667, 2014.

1153 Reimer, P. J., Bard, E., Bayliss, A., Beck, J. W., Blackwell, P. G., Bronk Ramsey, C., Buck, C. E.,
1154 Cheng, H., Edwards, R. L., Friedrich, M., Grootes, P. M., Guilderson, T. P., Haflidason, H., Hajdas, I.,
1155 Hatté, C., Heaton, T. J., Hoffmann, D. L., Hogg, A. G., Hughen, K. A., Kaiser, K. F., Kromer, B.,

1156 Manning, S. W., Niu, M., Reimer, R. W., Richards, D. A., Scott, E. M., Southon, J. R., Staff, R. A.,
1157 Turney, C. S. M., and van der Plicht, J.: IntCal13 and Marine13 Radiocarbon Age Calibration Curves
1158 0–50,000 Years cal BP, *Radiocarbon*, 55, 1869-1887, 2013.

1159 Rella, S. F., Tada, R., Nagashima, K., Ikehara, M., Itaki, T., Ohkushi, K., Sakamoto, T., Harada, N., and
1160 Uchida, M.: Abrupt changes of intermediate water properties on the northeastern slope of the Bering
1161 Sea during the last glacial and deglacial period, *Paleoceanography*, 27, PA3203,
1162 doi:3210.1029/2011pa002205, 2012.

1163 Riethdorf, J.-R., Max, L., Nuernberg, D., Lembke-Jene, L., and Tiedemann, R.: Deglacial development
1164 of (sub) sea surface temperature and salinity in the subarctic northwest Pacific: Implications for
1165 upper-ocean stratification, *Paleoceanography*, 28, doi:10.1002/palo.20014, 2013.

1166 Riethdorf, J.-R., Thibodeau, B., Ikehara, M., Nürnberg, D., Max, L., Tiedemann, R., and Yokoyama, Y.:
1167 Surface nitrate utilization in the Bering sea since 180ka BP: Insight from sedimentary nitrogen
1168 isotopes, *Deep Sea Research Part II: Topical Studies in Oceanography*, 125-126, 163-176, 2016.

1169 Rippert, N., Max, L., Mackensen, A., Cacho, I., Povea, P., and Tiedemann, R.: Alternating Influence of
1170 Northern Versus Southern-Sourced Water Masses on the Equatorial Pacific Subthermocline During the
1171 Past 240 ka, *Paleoceanography*, 32, 1256-1274, 2017.

1172 Rodríguez-Sanz, L., Mortyn, P. G., Herguera, J. C., and Zahn, R.: Hydrographic changes in the tropical
1173 and extratropical Pacific during the last deglaciation, *Paleoceanography*, 28, 529-538, 2013.

1174 Saenko, O. A., Schmittner, A., and Weaver, A. J.: The Atlantic-Pacific seesaw, *Journal of Climate*, 17,
1175 2033-2038, 2004.

1176 Sagawa, T. and Ikehara, K.: Intermediate water ventilation change in the subarctic northwest Pacific
1177 during the last deglaciation, *Geophysical Research Letters*, 35, 5, doi: 10.1029/2008gl035133, 2008.

1178 Scott, C. and Lyons, T. W.: Contrasting molybdenum cycling and isotopic properties in euxinic versus
1179 non-euxinic sediments and sedimentary rocks: Refining the paleoproxies, *Chemical Geology*, 324–325,
1180 19-27, 2012.

1181 Scott, C., Lyons, T. W., Bekker, A., Shen, Y., Poulton, S. W., Chu, X., and Anbar, A. D.: Tracing the
1182 stepwise oxygenation of the Proterozoic ocean, *Nature*, 452, 456-459, 2008.

1183 Shao, H., Yang, S., Cai, F., Li, C., Liang, J., Li, Q., Hyun, S., Kao, S.-J., Dou, Y., Hu, B., Dong, G., and
1184 Wang, F.: Sources and burial of organic carbon in the middle Okinawa Trough during late Quaternary
1185 paleoenvironmental change, *Deep Sea Research Part I: Oceanographic Research Papers*, 118, 46-56,
1186 2016.

1187 Shcherbina, A. Y., Talley, L. D., and Rudnick, D. L.: Direct observations of North Pacific ventilation:
1188 Brine rejection in the Okhotsk Sea, *Science*, 302, 1952-1955, 2003.

1189 Shi, X., Wu, Y., Zou, J., Liu, Y., Ge, S., Zhao, M., Liu, J., Zhu, A., Meng, X., Yao, Z., and Han, Y.:
1190 Multiproxy reconstruction for Kuroshio responses to northern hemispheric oceanic climate and the
1191 Asian Monsoon since Marine Isotope Stage 5.1 (~88 ka), *Climate of the Past*, 10, 1735-1750, 2014.

1192 Shibahara, A., Ohkushi, K., Kennett, J. P., and Ikehara, K.: Late Quaternary changes in intermediate
1193 water oxygenation and oxygen minimum zone, northern Japan: A benthic foraminiferal perspective,
1194 *Paleoceanography*, 22, PA3213, doi:3210.1029/2005pa001234, 2007.

1195 Shimmiel, G. B. and Price, N. B.: The behaviour of molybdenum and manganese during early
1196 sediment diagenesis — offshore Baja California, Mexico, *Marine Chemistry*, 19, 261-280, 1986.

1197 Sibuet, J. C., Letouzey, J., Barbier, F., Charvet, J., Foucher, J. P., Hilde, T. W. C., Kimura, M., Chiao,
1198 L.-Y., Marsset, B., Muller, C., and Stéphan, J. F.: Back Arc Extension in the Okinawa Trough, *Journal
1199 of Geophysical Research: Solid Earth*, 92, 14041-14063, 1987.

1200 Sigman, D. M. and Boyle, E. A.: Glacial/interglacial variations in atmospheric carbon dioxide, *Nature*,
1201 407, 859-869, 2000.

1202 Spratt, R. M. and Lisiecki, L. E.: A Late Pleistocene sea level stack, *Clim. Past*, 12, 1079-1092, 2016.

1203 Sun, Y., Clemens, S. C., Morrill, C., Lin, X., Wang, X., and An, Z.: Influence of Atlantic meridional
1204 overturning circulation on the East Asian winter monsoon, *Nature Geosci*, 5, 46-49, 2012.

1205 Sun, Y. B., Oppo, D. W., Xiang, R., Liu, W. G., and Gao, S.: Last deglaciation in the Okinawa Trough:
1206 Subtropical northwest Pacific link to Northern Hemisphere and tropical climate, *Paleoceanography*, 20,
1207 PA4005, doi:4010.1029/2004pa001061, 2005.

1208 Sundby, B., Martinez, P., and Gobeil, C.: Comparative geochemistry of cadmium, rhenium, uranium,
1209 and molybdenum in continental margin sediments, *Geochimica et Cosmochimica Acta*, 68, 2485-2493,
1210 2004.

1211 Talley, L. D.: Distribution foramtion of North Pacific Intermediate water, *Journal of Physical*
1212 *Oceanography*, 23, 517-537, 1993.

1213 Talley, L. D.: Hydrographic Atlas of the World Ocean Circulation Experiment (WOCE). In: Volume 2:
1214 Pacific Ocean, Sparrow, M., Chapman, P., and Gould, J. (Eds.), International WOCE Project Office,
1215 Southampton, UK, 2007.

1216 Tribouillard, N., Algeo, T. J., Lyons, T., and Riboulleau, A.: Trace metals as paleoredox and
1217 paleoproductivity proxies: An update, *Chemical Geology*, 232, 12-32, 2006.

1218 Ujiié, H. and Ujiié, Y.: Late Quaternary course changes of the Kuroshio Current in the Ryukyu Arc
1219 region, northwestern Pacific Ocean, *Marine Micropaleontology*, 37, 23-40, 1999.

1220 Ujiié, Y., Asahi, H., Sagawa, T., and Bassinot, F.: Evolution of the North Pacific Subtropical Gyre
1221 during the past 190 kyr through the interaction of the Kuroshio Current with the surface and
1222 intermediate waters, *Paleoceanography*, 31, 1498-1513, 2016.

1223 Ujiié, Y., Ujiié, H., Taira, A., Nakamura, T., and Oguri, K.: Spatial and temporal variability of surface
1224 water in the Kuroshio source region, Pacific Ocean, over the past 21,000 years: evidence from
1225 planktonic foraminifera, *Marine Micropaleontology*, 49, 335-364, 2003.

1226 Vorlicek, T. P. and Helz, G. R.: Catalysis by mineral surfaces: Implications for Mo geochemistry in
1227 anoxic environments, *Geochimica et Cosmochimica Acta*, 66, 3679-3692, 2002.

1228 Wahyudi and Minagawa, M.: Response of benthic foraminifera to organic carbon accumulation rates in
1229 the Okinawa Trough, *Journal of Oceanography*, 53, 411-420, 1997.

1230 Wan, S. and Jian, Z.: Deep water exchanges between the South China Sea and the Pacific since the last
1231 glacial period, *Paleoceanography*, 29, 1162-1178, 2014.

1232 Wang, Y., Cheng, H., Edwards, R. L., He, Y., Kong, X., An, Z., Wu, J., Kelly, M. J., Dykoski, C. A.,
1233 and Li, X.: The Holocene Asian Monsoon: Links to Solar Changes and North Atlantic Climate, *Science*,
1234 308, 854-857, 2005.

1235 Wu, Y., Cheng, Z., and Shi, X.: Stratigraphic and carbonate sediment characteristics of Core CSH1
1236 from the northern Okinawa Trough, *Advances in Marine Science*, 22, 163-169 (in Chinese with English
1237 Abstract), 2004.

1238 Wu, Y., Shi, X., Zou, J., Cheng, Z., Wang, K., Ge, S., and Shi, F.: Benthic foraminiferal $\delta^{13}C$
1239 minimum events in the southeastern Okhotsk Sea over the last 180ka, *Chinese Science Bulletin*, 59,
1240 3066-3074, 2014.

1241 You, Y. Z.: The pathway and circulation of North Pacific Intermediate Water, *Geophysical Research*
1242 *Letters*, 30, doi:10.1029/2003gl018561, 2003.

1243 You, Y. Z., Suginozawa, N., Fukasawa, M., Yasuda, I., Kaneko, I., Yoritaka, H., and Kawamiya, M.:

1244 Roles of the Okhotsk Sea and Gulf of Alaska in forming the North Pacific Intermediate Water, *Journal*
1245 *of Geophysical Research-Oceans*, 105, 3253-3280, 2000.

1246 You, Y. Z., Suginothara, N., Fukasawa, M., Yoritaka, H., Mizuno, K., Kashino, Y., and Hartoyo, D.:
1247 Transport of North Pacific Intermediate Water across Japanese WOCE sections, *Journal of Geophysical*
1248 *Research-Oceans*, 108, doi: 10.1029/2002jc001662, 2003.

1249 Yu, H., Liu, Z. X., Berne, S., Jia, G. D., Xiong, Y. Q., Dickens, G. R., Wei, G. J., Shi, X. F., Liu, J. P.,
1250 and Chen, F. J.: Variations in temperature and salinity of the surface water above the middle Okinawa
1251 Trough during the past 37 kyr, *Palaeogeography Palaeoclimatology Palaeoecology*, 281, 154-164,
1252 2009.

1253 Zhang, X., Knorr, G., Lohmann, G., and Barker, S.: Abrupt North Atlantic circulation changes in
1254 response to gradual CO₂ forcing in a glacial climate state, *Nature Geoscience*, 10, 518-524, 2017.

1255 Zheng, X., Kao, S., Chen, Z., Menviel, L., Chen, H., Du, Y., Wan, S., Yan, H., Liu, Z., Zheng, L., Wang,
1256 S., Li, D., and Zhang, X.: Deepwater circulation variation in the South China Sea since the Last Glacial
1257 Maximum, *Geophysical Research Letters*, 43, 8590-8599, 2016.

1258 Zheng, Y., Anderson, R., van Geen, A., and Fleisher, M.: Remobilization of authigenic uranium in
1259 marine sediments by bioturbation, *Geochimica et Cosmochimica Acta*, 66, 1759-1772, 2002.

1260 Zheng, Y., Anderson, R., van Geen, A., and Kuwabara, J.: Authigenic molybdenum formation in marine
1261 sediments: a link to pore water sulfide in the Santa Barbara Basin, *Geochimica et Cosmochimica Acta*,
1262 64, 4165-4178, 2000.

1263 Zhu, A., Shi, X., Zou, J., Wu, Y., Zhang, H., and Bai, Y.: Sediment Provenance and Fluxes in the
1264 Northern Okinawa Trough During the last 88ka, *Marine Geology & Quaternary Geology*, 35, 1-8 (in
1265 Chinese with English Abstract), 2015.

1266 Zou, J., Shi, X., Liu, Y., Liu, J., Selvaraj, K., and Kao, S.-J.: Reconstruction of environmental changes
1267 using a multi-proxy approach in the Ulleung Basin (Sea of Japan) over the last 48 ka, *Journal of*
1268 *Quaternary Science*, 27, 891-900, 2012.

1269

1270 **Captions**

1271 **Table 1.** Locations of different sediment core records and their source references
1272 discussed in the text.

带格式的: 两端对齐

1273

1274 **Table 2.** Age control points adopted between planktic foraminifera species
1275 *Globigerinoides ruber* $\delta^{18}\text{O}$ of Core CSH1 and Chinese stalagmite $\delta^{18}\text{O}$ (Cheng et al.,
1276 2016) for tuning the age model between 10 ka and 60 ka in this study. A linear
1277 interpolation was assumed between age control points.

带格式的: 字体: 倾斜

1278

1279 **Figure 1.** (a) Spatial distribution of dissolved oxygen content at 700 m water depth in
1280 the North Pacific. Black arrows denote simplified Kuroshio and Oyashio circulations
1281 and North Pacific Intermediate Water (NPIW) in the North Pacific. The red thick
1282 dashed line indicates transformation of Okhotsk Sea Intermediate Water (OSIW) by
1283 cabbeling the subtropical NPIW along the subarctic-tropical frontal zone (You, 2003).

域代码已更改

1284 The light brown solid line with arrow indicates the spreading path of subtropical
1285 NPIW from northeast North Pacific southward toward the low-latitude northwest
1286 North Pacific (You, 2003). Yellow solid lines with arrow represent two passages

域代码已更改

1287 through which NPIW enter into the Okinawa Trough. This figure was created with
1288 Ocean Data View (odv.awi.de). (b) Location of sediment core CSH1 investigated in
1289 this study (red diamond). Also shown are locations of sediment cores PN-3, E017, 255
1290 and MD012404 investigated previously from the Okinawa Trough, GH08-2004 from
1291 the East of Ryukyu Island, GH02-1030 off ~~(PN-3, E017, 255 and MD012404; white~~
1292 ~~cross line), the east of Japan~~ ~~northern and southern Japan (GH08-2004 and~~
1293 ~~GH02-1030), PC-23A from~~ the Bering Sea ~~(PC-23A)~~ and ODP167-1017 from the
1294 northeastern Pacific ~~(ODP167-1017)~~. Letters A to E represent the sediment cores from
1295 and near the OT. The detailed information for these cores ~~can be seen~~ is shown in
1296 Table 1.

1297

1298 **Figure 2.** Spatial distribution of sea surface salinity in the East China Sea. (a) summer
1299 (July to September); (b) winter (January to March). Lower sea surface salinity in

1300 summer relative to that of winter indicates strong effects of summer East Asian
1301 Monsoon.

1302

1303 **Figure 3.** (a) Lithology and oxygen isotope ($\delta^{18}\text{O}$) profile of planktic foraminifera
1304 species *Globigerinoides ruber* (*G.ruber*) in core CSH1. (b) Plot of ages versus depth
1305 for core CSH1. Three known ash layers are indicated by solid red rectangles. (c) Time
1306 series of linear sedimentation rate (LSR) from core CSH1. (d) Comparison of age
1307 model of core CSH1 with Chinese Stalagmite composite $\delta^{18}\text{O}$ curve of (Cheng et al.,
1308 2016). Tie points for CSH1 core chronology (Table 2) in Figures 2b-3c and 2e-3d are
1309 designated by blue and red solid colored dots/crosses.

1310

1311 **Figure 4.** Age versus (a) CaCO₃ concentration, linear sedimentation rate (LSR), (b)
1312 Total nitrogen (TN) concentration, C/N molar ratio, (c) Total organic carbon (TOC)
1313 concentration, (d) C/N molar ratio, Total nitrogen (TN) concentration, (e) linear
1314 sedimentation rate (LSR), CaCO₃ concentration, (f) Al concentration, (g) Mn
1315 concentration, (h) Mo/Mn ratio, (i) Mo concentration, (j) excess Mo concentration, (k)
1316 U concentration and (l) excess U concentration and (m) (Mo/U)_{excess} ratio in core
1317 CSH1. Light gray and dark gray~~Gray and black~~ vertical bars indicate different
1318 sediment intervals in core CSH1. ~~MIS indicates Marine Isotope Stage~~. 8.2 ka, PB, YD,
1319 B/A, HS1, LGM and HS2 refer to 8,200 year cold event, Preboreal, Younger Dryas,
1320 Bölling - Alleröd, Heinrich Stadial 1, Last Glacial Maximum and Heinrich Stadial 2,
1321 respectively, which were identified in core CSH1. Blue solid diamonds in Figure ~~3l~~
1322 4m indicate the age control points.

1323

1324 **Figure 5.** Scatter plots of Mo_{excess} vs Mn concentrations and U_{excess} concentration vs
1325 Mo/Mn ratio at different time intervals in core CSH1. A various correlation is present
1326 in core CSH1 at different time intervals, which shows their complicated geochemical
1327 behaviors (Figs.5a and 5b). Strong positive correlation between U_{excess} concentration
1328 and Mo/Mn ratio and U_{excess} concentration (Fig.5c) suggest that Mo/Mn ratio they are
1329 is a reliable proxy suitable to track sedimentary redox conditions in the geological

域代码已更改

带格式的: 字体: 五号

带格式的: 下标

1330 past.

1331

1332 **Figure 6.** Proxy-related reconstructions of ~~intermediate water~~mid-depth sedimentary
1333 oxygenation at site CSH1 (this study) compared with oxygenation records from other
1334 locations of the North Pacific and published climatic and environmental records from
1335 the Okinawa Trough. From top to bottom: (a) CaCO₃ concentration, (b) U_{excess}
1336 concentration, (c) Mo/Mn ratio, and (d) ~~Mn concentration~~sea surface temperature
1337 (SST-) (Shi et al., 2014), ~~and~~ (e) abundance of *P.obliquiloculata* in core CSH1 (Shi et
1338 al., 2014) ~~and~~, (f) bulk sedimentary organic matter $\delta^{15}\text{N}$ ~~of TOC~~ in core MD01-2404
1339 (Kao et al., 2008), (g) $\delta^{13}\text{C}$ of epibenthic foraminiferal *C.wuellerstorfi* in core PN-3
1340 (Wahyudi and Minagawa, 1997), (h) relative abundance of *B. aculeata* (hypoxia-like
1341 species) and (i) *C. hyalinaea* (oxygen-like species) (Li et al., 2005), (hj) Dysoxic
1342 dysoxic taxa (%) in core ODP 167-1017 in the northeastern Pacific (Cannariato and
1343 Kennett, 1999) and ~~(k)~~ $\delta^{13}\text{C}$ of benthic foraminiferal *Uvigerina akitaensis* in core
1344 PC23A in the Bering Sea (Rella et al., 2012). Light gray ~~Gray~~ and dark gray ~~black~~
1345 vertical bars are the same as those in Figure 4.

1346

1347 **Figure 7.** Proxy records favoring the existence of out-of-phase connections ~~oceanic~~
1348 ~~ventilation seesaw~~ between the subtropical North Pacific and North Atlantic during
1349 the last deglaciation and enhanced carbon storage at mid-depth waters. (a) U_{excess}
1350 concentration in core CSH1; Atmospheric CO₂ concentration (Marcott et al., 2014) (b)
1351 Mo/Mn ratio in core CSH1; Indicator of strength of Atlantic Meridional Ocean
1352 Circulation (²³¹Pa/²³⁰Th) (Böhm et al., 2015; McManus et al., 2004); (c) benthic $\delta^{13}\text{C}$
1353 record in core PC-23A in the Bering Sea (Rella et al., 2012); (d) Indicator of strength
1354 of Atlantic Meridional Ocean Circulation (²³¹Pa/²³⁰Th) (Böhm et al., 2015; McManus
1355 et al., 2004); Mo/Mn ratio in core CSH1; (e) Atmospheric CO₂ concentration (Marcott
1356 et al., 2014) U_{excess} concentration in core CH1. Light gray and dark gray vertical bars
1357 are the same as those in Figure 4. Blue diamonds are the same as those in Figure 3.

1358

域代码已更改

域代码已更改

带格式的: 字体: 倾斜

域代码已更改

带格式的: 字体: 倾斜

域代码已更改

Table 1

Label in Figure 1b	Station	Latitude_(°N)	Longitude_(°E)	Water depth (m)	Area	Reference
	CSH1	31.23	128.72	703	Okinawa Trough	this study
A	PN-3	28.10	127.34	1058	Okinawa Trough	Wahyudi and Minagawa, (1997)
B	MD012404	26.65	125.81	1397	Okinawa Trough	Kao et al., (2008)
C	E017	26.57	126.02	1826	Okinawa Trough	Li et al., (2005)
D	255	25.20	123.12	1575	Okinawa Trough	Jian et al., (1996)
E	GH08-2004	26.21	127.09	1166	East of Ryukyu Island	Kubota et al. (2010,2015)
	GH02-1030	42.23	144.21	1212	Off Japan	Sagawa and Ikehara, (2008)
	PC-23A	60.16	179.46	1002	Bering Sea	Rella et al.,(2012)
	ODP167-1017	34.54	239.11	955	NE Pacific	Cannariato and Kennett, (1999)

带格式的：两端对齐

带格式的：居中

带格式表格

带格式的：两端对齐

带格式的：段落间距段前：0 磅，段后：0 磅，行距：单倍行距，与下段不同页，段中分页

带格式的：居中

带格式表格

带格式的：居中

带格式的：居中

带格式的：居中

带格式的：居中

带格式的：段落间距段前：0 磅，段后：0 磅，行距：单倍行距，与下段不同页，段中分页

带格式的：段落间距段前：0 磅，段后：0 磅，行距：单倍行距，与下段不同页，段中分页

带格式的：到齐到网格，制表位：不在 19.78 字符 + 39.55 字符

带格式的：段落间距段前：0 磅，段后：0 磅，行距：单倍行距，与下段不同页，段中分页

1
2

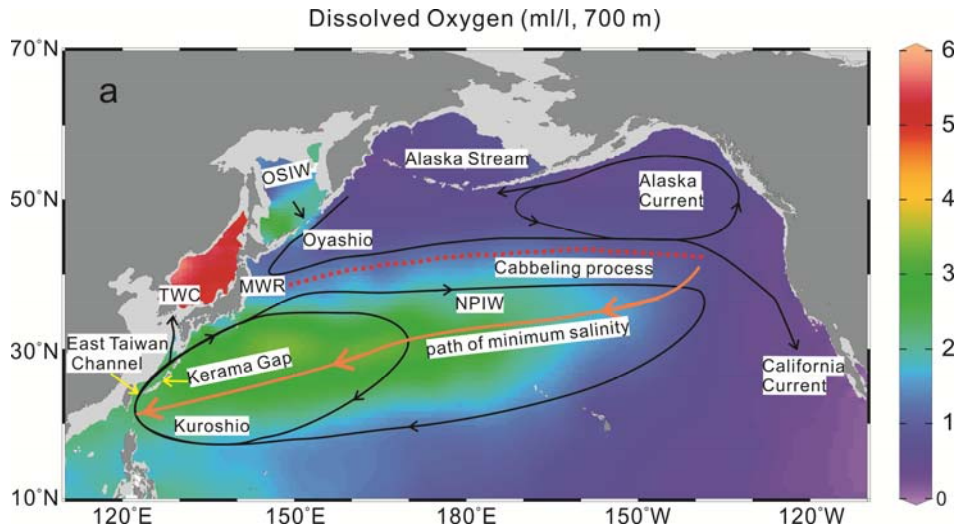
Table 2

Depth(cm)	AMS ¹⁴ C (yr)	Error (yr)	Calibrated Age (yr)	Tie Point Type	LSR (cm/ka)	Source
10	3420	±35	3296	¹⁴ C		Shi et al., (2014)
106	7060	± 40	7545	¹⁴ C	22.59	Shi et al., (2014)
218			12352	Stalagmite, YD	23.30	This study
322			16029	Stalagmite, H1	28.28	This study
362			19838	Stalagmite	10.50	This study
466			23476	Stalagmite, DO2	28.59	This study
506			24163	Stalagmite, H2	58.22 <u>33.29</u>	This study
698			28963	Stalagmite, DO4	40.00	This study
746			29995	Stalagmite, H3	46.51	This study
834			32442	Stalagmite, DO5	35 <u>39.09</u> <u>96</u>	This study
938			37526	Stalagmite, DO8	20.46	This study
978			39468	Stalagmite, H4	20.60	This study
1058			46151	Stalagmite, DO12	11.97	This study
1122			49432	Stalagmite, DO13	19.51	This study
1242			52831	Stalagmite, DO14	35.30	This study
1282			57241	Stalagmite, DO16	9.07	This study
1346			61007	Stalagmite, H6	16.99	This study
1530		±2590	73910	MIS4/5	14.26	Shi et al., (2014)
1610		±3580	79250	MIS 5.1	14.98	Shi et al., (2014)

3
4
5

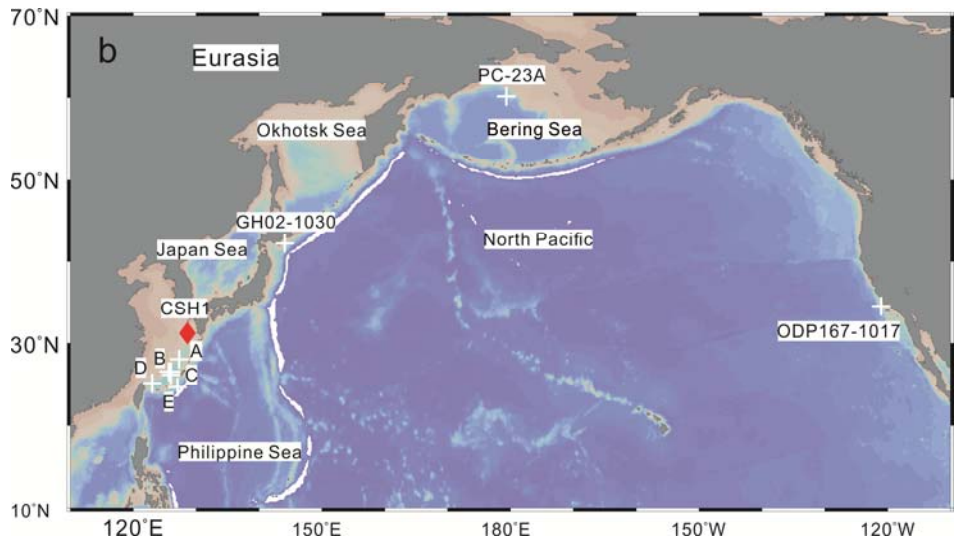
- 带格式的 ... [1]
- 带格式的 ... [2]
- 带格式的 ... [3]
- 带格式的 ... [4]
- 带格式的 ... [5]
- 带格式的 ... [6]
- 带格式的 ... [7]
- 带格式的 ... [8]
- 带格式的 ... [9]
- 带格式的 ... [10]
- 带格式的 ... [11]
- 带格式的 ... [12]
- 带格式的 ... [13]
- 带格式的 ... [14]
- 带格式的 ... [15]
- 带格式的 ... [16]
- 带格式的 ... [17]
- 带格式的 ... [18]
- 带格式的 ... [19]
- 带格式的 ... [20]
- 带格式的 ... [21]
- 带格式的 ... [22]
- 带格式的 ... [23]
- 带格式的 ... [24]
- 带格式的 ... [25]
- 带格式的 ... [26]
- 带格式的 ... [27]
- 带格式的 ... [28]
- 带格式的 ... [29]
- 带格式的 ... [30]
- 带格式的 ... [31]
- 带格式的 ... [32]
- 带格式的 ... [33]
- 带格式的 ... [34]
- 带格式的 ... [35]
- 带格式的 ... [36]
- 带格式的 ... [37]
- 带格式的 ... [38]
- 带格式的 ... [39]
- 带格式的 ... [40]
- 带格式的 ... [41]
- 带格式的 ... [42]
- 带格式的 ... [43]
- 带格式的 ... [44]
- 带格式的 ... [45]
- 带格式的 ... [46]
- 带格式的 ... [47]
- 带格式的 ... [48]
- 带格式的 ... [49]
- 带格式的 ... [50]
- 带格式的 ... [51]
- 带格式的 ... [52]
- 带格式的 ... [53]

6 Fig.1



7

8

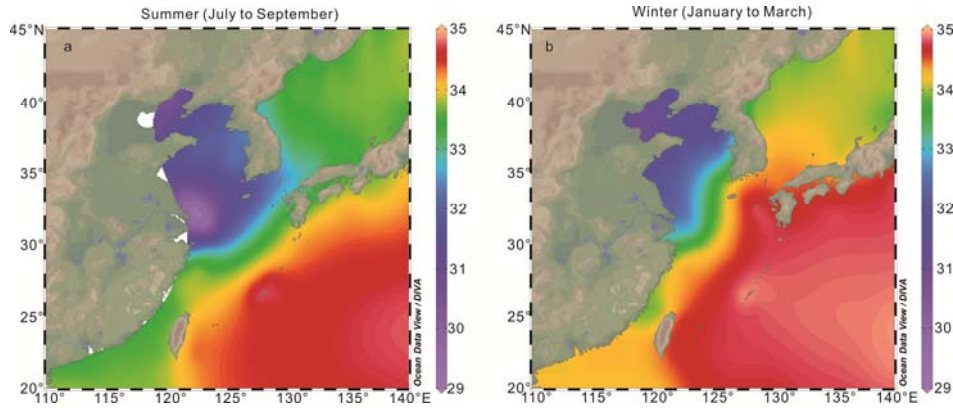


9

10

11

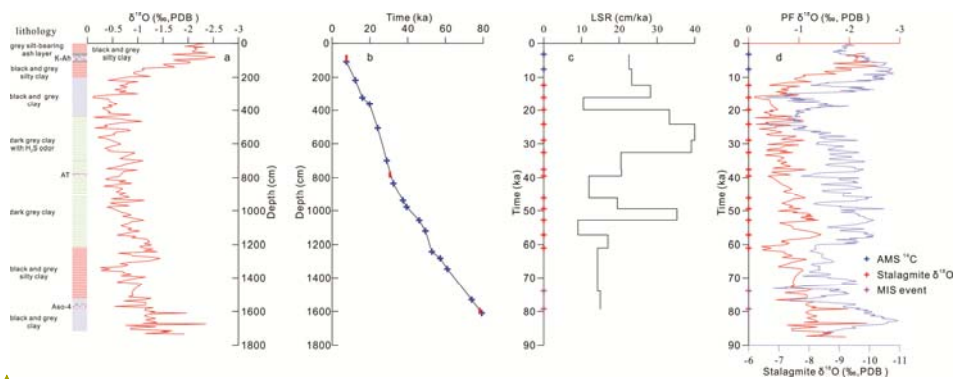
12 Fig.2



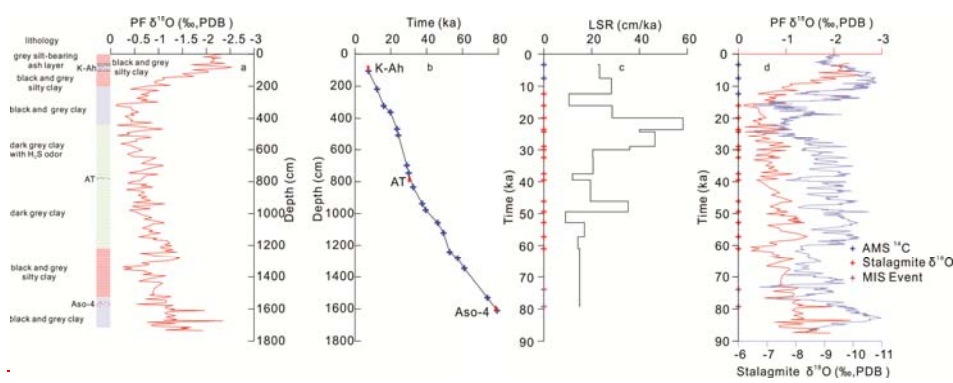
13

14

15 Fig.3



16



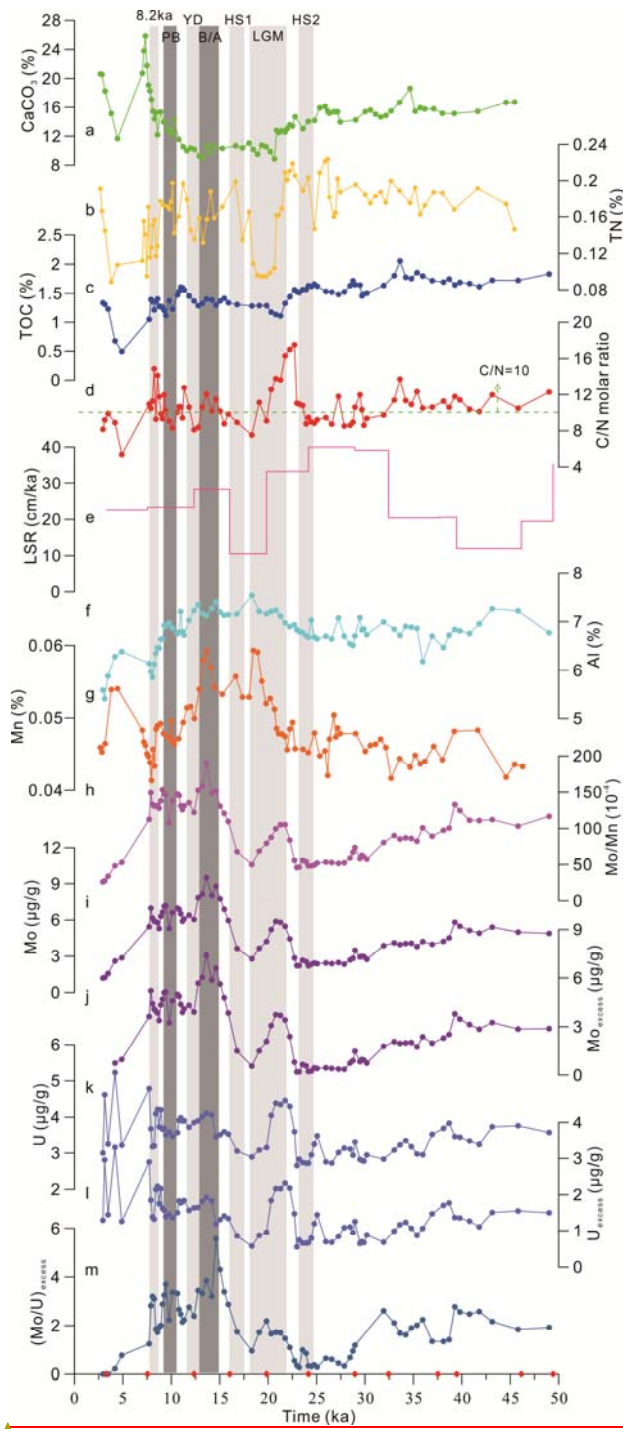
17

18

19

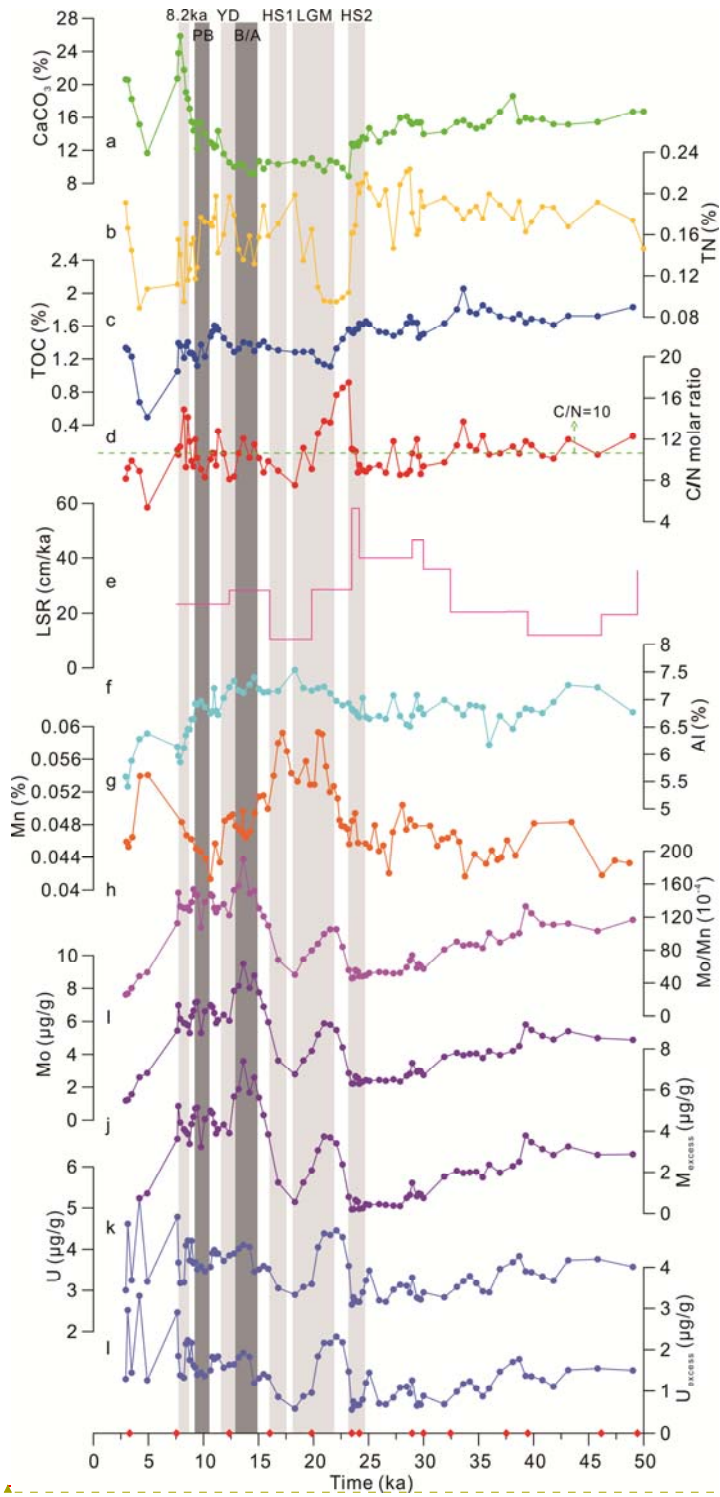
带格式的: 字体: 小四

20 Fig.4



21

带格式的: 字体: 小四

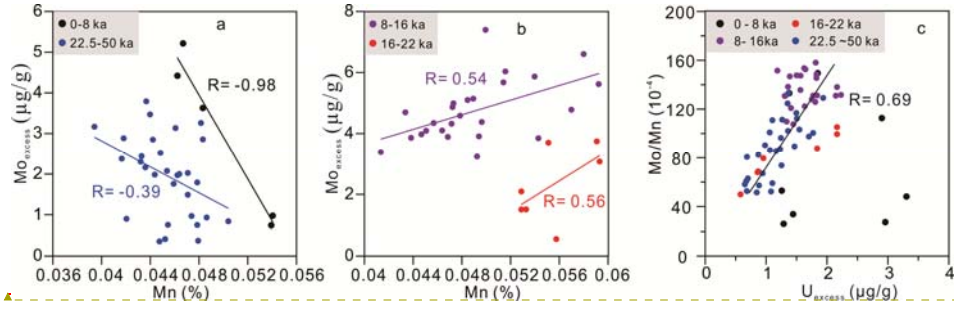


带格式的: 字体: 小四

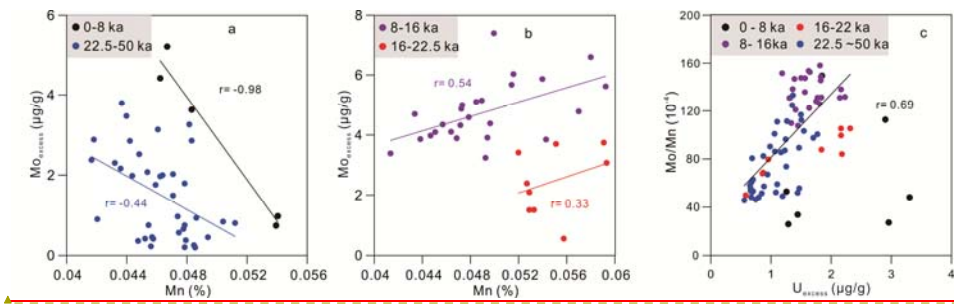
23

24

25 Fig.5



26



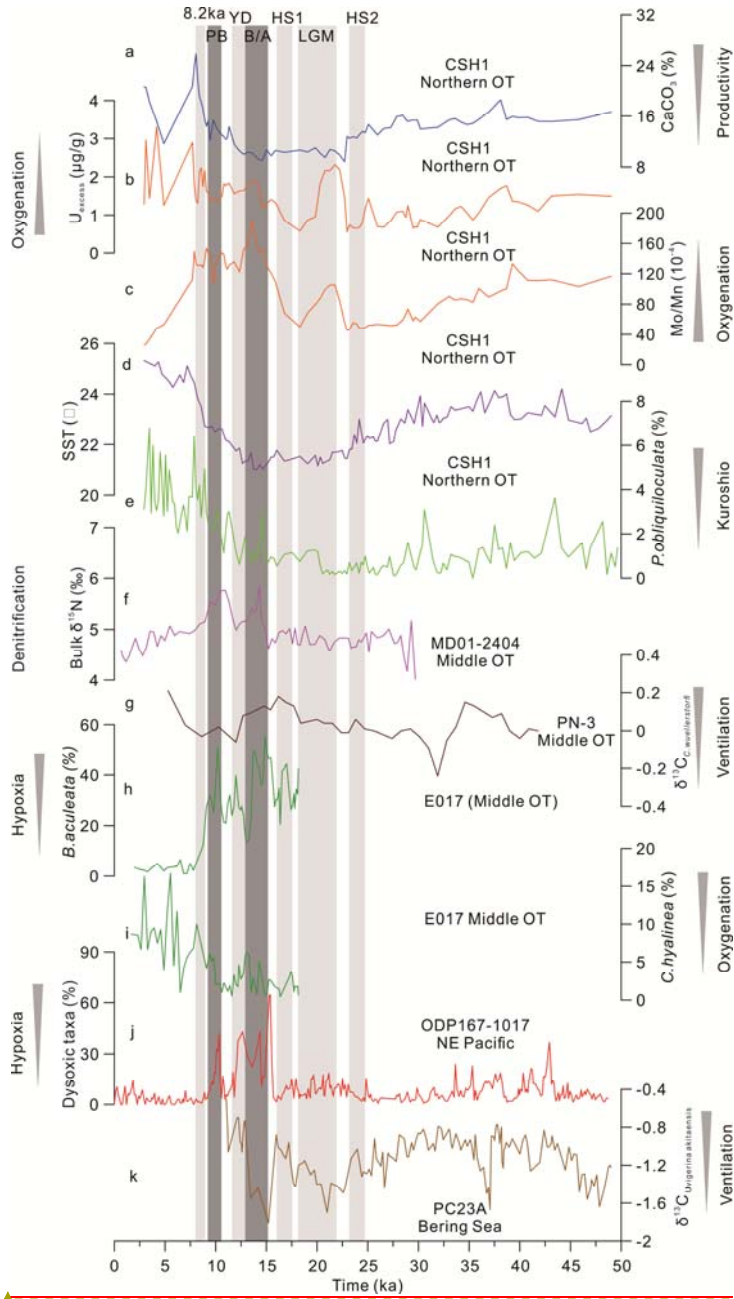
27

28

带格式的: 字体: 小四

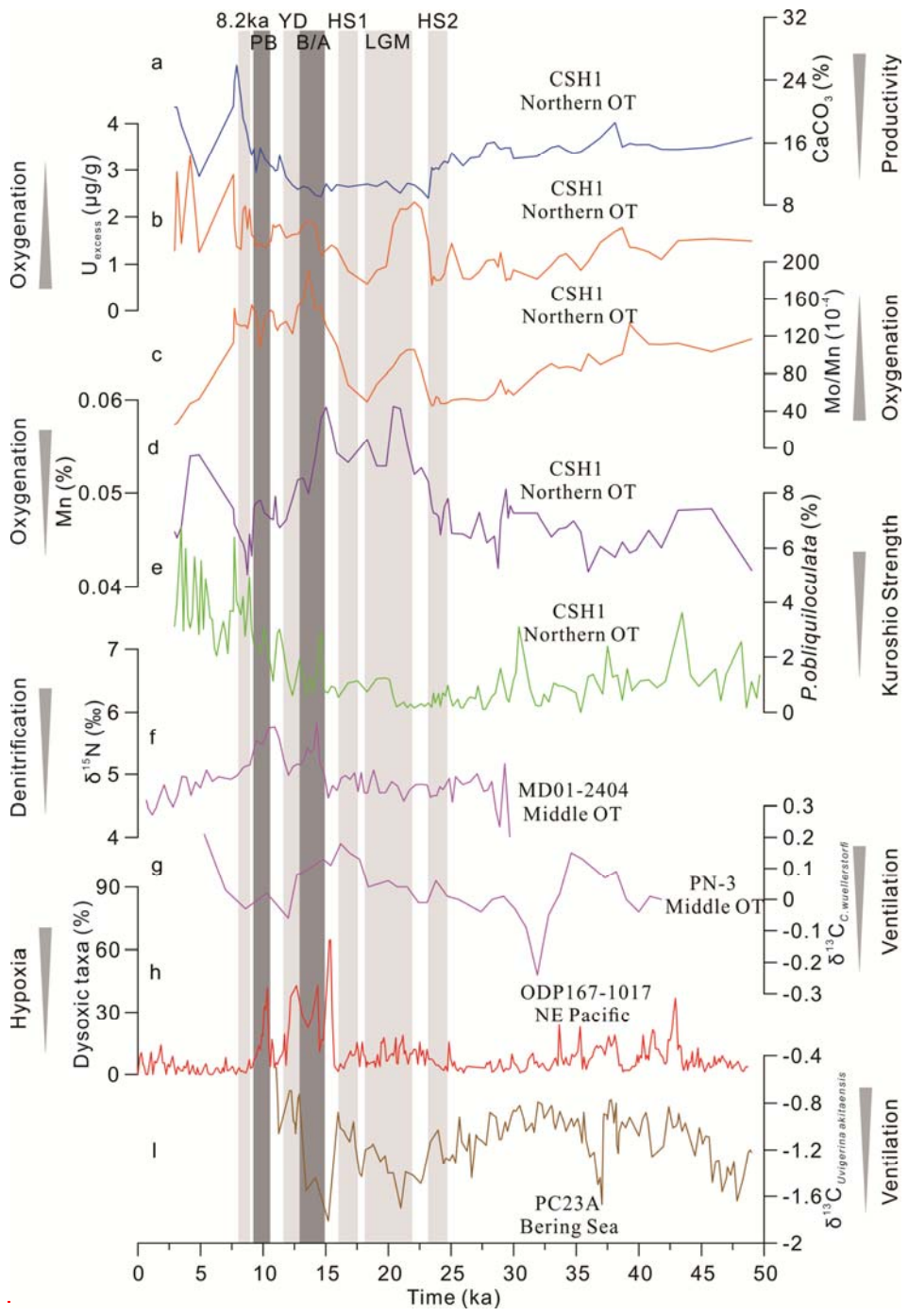
带格式的: 字体: 小四

29 Fig.6



30

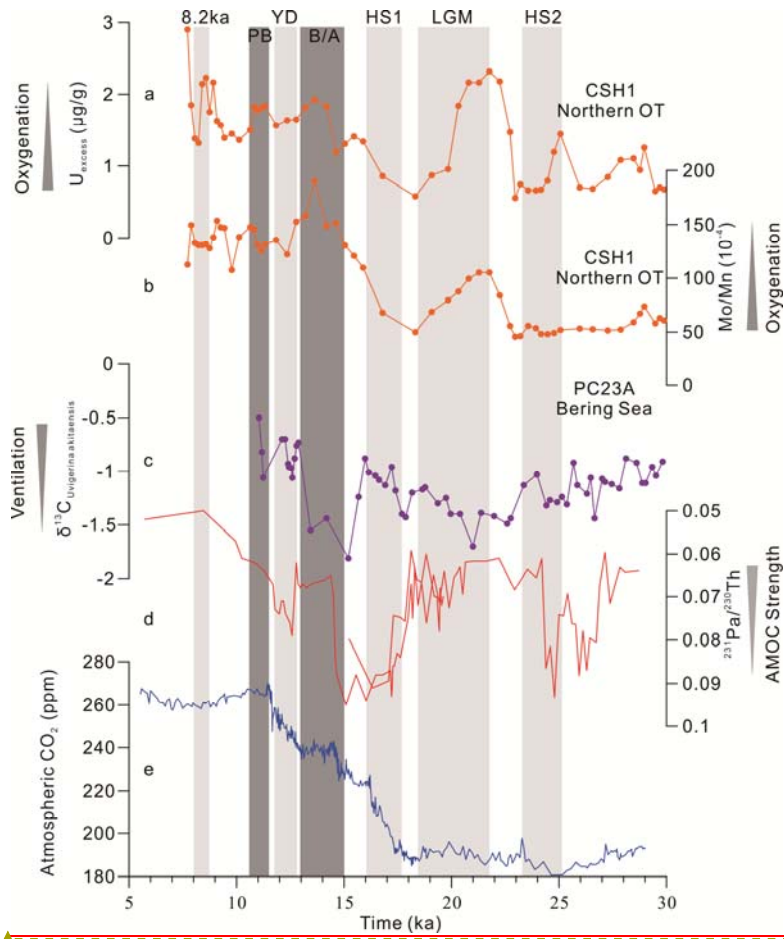
带格式的: 字体: 小四



31

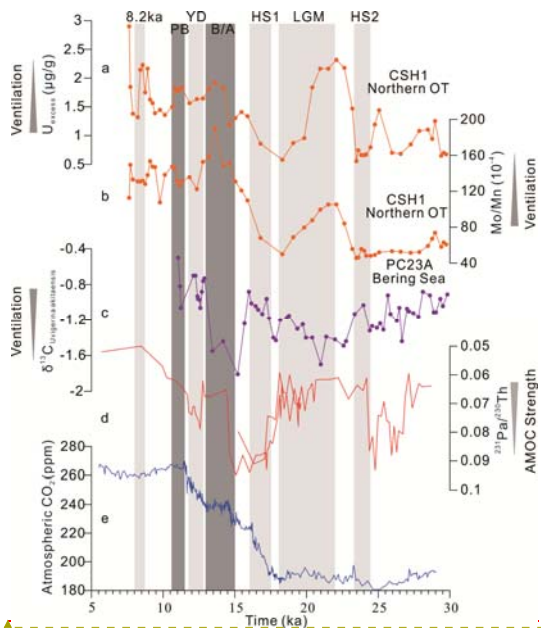
32

33 Fig.7



34

带格式的: 字体: 小四



带格式的: 字体: 小四